2022

EVALUATING THE USE OF CAMERA TRAPS TO MONITOR POPULATIONS OF UNGULATE PREY IN THE RUSSIAN FAR EAST

Scott Johnston Waller

Jedediah Brodie
University of Montana, Missoula

Dale G. Miquelle
Wildlife Conservation Society

Hugh Robinson
Panthera

Mark Hebblewhite
University of Montana - Missoula

EVALUATING THE USE OF CAMERA TRAPS TO MONITOR POPULATIONS OF UNGULATE PREY IN THE RUSSIAN FAR EAST

By

SCOTT JOHNSTON WALLER

B.A., Middlebury College, Middlebury, Vermont, 2018

Thesis

presented in partial fulfillment of the requirements
for the degree of

Master of Science
in Wildlife Biology

The University of Montana
Missoula, MT

May 2022

Approved by:

Scott Whittenburg, Dean of The Graduate School
Graduate School

Dr. Mark Hebblewhite, Co-Chair
Wildlife Biology Program, Department of Ecosystem and Conservation Sciences

Dr. Jedediah Brodie, Co-Chair
Wildlife Biology Program, Department of Biological Sciences

Dr. Hugh Robinson
Wildlife Biology Program; Director, Landscape Analysis Lab, Panthera

Dr. Dale Miquelle
Director, Wildlife Conservation Society Russia Program

Waller, Scott, M.S., May 2022 Wildlife Biology

Evaluating the Use of Camera Traps to Monitor Prey Populations in the Russian Far East

Co-Chairperson: Dr. Mark Hebblewhite

Co-Chairperson: Dr. Jedediah Brodie

ABSTRACT

Efforts to recover endangered carnivore populations are often limited by insufficient populations of prey. When recovering prey populations, estimates of population density are invaluable metrics to monitor recovery efforts. In Russia, wildlife managers use the Formozov-Malyushev-Pereleshin (FMP) snow tracking method to estimate densities of ungulate prey of the Amur tiger (*Panthera tigris*). Yet, increasing variability in snow conditions and other challenges have limited its reliability. Camera traps offer a promising alternative approach since managers already use cameras to monitor tigers. However, the assumptions and study design necessary to implement capture-recapture models for tigers are different from those needed to implement models for unmarked populations of prey. In Chapter 1, I estimated densities of wild boar (*Sus scrofa*), red deer (*Cervus canadensis* ssp. *xanthopygus*), roe deer (*Capreolus pygargus*), and sika deer (*Cervus nippon*) using Random Encounter models (REM), Space-To-Event models (STE), and Time-To-Event models (TTE), then compared these with FMP estimates within Sikhote-Alin Biosphere Zapovednik. Estimates from the STE and FMP were the most similar, though there were challenges implementing the STE to data from motion-trigger cameras. All models detected a >90% decline in wild boar density due to African Swine Fever. Simulations indicated that greater survey effort for all camera-based methods would be required to achieve a coefficient of variation of 20% (an objective set for this study area in 2006). This is likely cost-prohibitive for many conservation programs due to the high costs of randomly deploying many cameras. To examine the influence of study design on detections of ungulate prey, in Chapter 2 I compared relative abundance indices (RAIs) of prey using: (1) cameras placed on roads to monitor tigers; (2) cameras placed using systematic random sampling; and (3) “off-road” cameras placed 150 meters away from road cameras. Both road and off-road RAIs were greater than random RAIs, and our attempt to approximate representative sampling with off-road cameras ultimately did not work. These results highlight the importance of random sampling to meet the assumptions of unmarked estimators. Detection data of prey species from cameras placed for tiger monitoring should not be used to estimate true abundance of prey species using these models.

TABLE OF CONTENTS

ACKNOWLEDGEMENTS

Funding and support for this project was provided by the Wildlife Conservation Society (WCS), the University of Montana, the Minnesota Zoo, and Conservation Frontlines.

First and foremost, I would like to thank Dr. Dale Miquelle for taking a chance on me four years ago. I was just finishing my undergraduate degree and was eager to apply both my passion for conservation and 7-semesters' worth of Russian language study. Dale eventually invited me over as a volunteer for the WCS Russia program in the Fall of 2018. Little did I know this was the beginning of a love for the Russian Far East and the start of a new chapter in my life. Dale has shown me constant support, advice, and kindness these last four years. He even brought me fig bars. I could not ask for a better role model in conservation, and for that I thank you.

The rest of my committee members deserve thanks next: my advisors, Dr. Jedediah Brodie and Dr. Mark Hebblewhite, and my final committee member, Dr. Hugh Robinson. I'm so glad my persistent emails and door-knocking paid off back in the spring of 2019. Mark, I have never met a human with more knowledge at their fingertips than you. Jed, you completely redefined the word "cool" in my vocabulary and are an inspiring ecologist. Hugh, I always feel guilty when I come to your office because I still can't remember which way to turn coming down the stairs. You have always been ready to hear me out and offer sage advice. Thank you all for your support, guidance, and friendship these last three years. I cannot imagine having a better committee than you all.

This research project would not have existed without the full support and dedication of the WCS Russia staff. I would like to thank Marina Miquelle first for her mentorship and friendship. She has shown me more patience than I think anyone rightly deserves, and her ready laugh always lightens my spirit. She also brought me fig bars. All the WCS Russia field staff deserve a lifetime of thanks: Roman Nazarenko, Kristina Baradulina, Zhenya Gishko, Sergey Khramulev, Volodya

Melnikov, and Galya Kovach all worked tirelessly on this project. I'm afraid I've completely ruined the word *sluchaynyi* for them (Russian: случайный, random). Both Irina Vlasovna and Vova Bykov were essential to the success of this project.

Sergey Avdeyuk and Petya Mametev deserve statues erected in their honor. First, I want to thank Sergey for helping me with this project. He too took a risk when he agreed to help me, and I'm so grateful he did. He has taught me so much natural history of the Far East, and I don't think I'll ever meet a backcountry cook as good. I'm proud to have worked with you and call you my friend. When COVID-19 prevented me from returning to Russia for the 2020-21 season, Petya stepped in and worked tirelessly with Sergey. He has shown me nothing but support and is a fantastic wildlife and wild place photographer. Without the two of them, we would not have camera data from 2020-21. I owe you both of you a lifetime of quality American coffee and beer.

Though not in the field, I would like to thank the rest of the WCS Russia team. Sasha Reebin, for his help with my Russian and for providing many parables. My list of new Russian words explodes whenever we are together. Anton Semyonov, for his friendship since my first day in Russia. Who would have thought that a first night in Russia would consist of a bluegrass concert put on by a band from Portland? Katya Nikolaeva, for her help with translations and processing camera data. Andrei Dotsenko, Igor Kolodin, Natalia Karp, and Tanya Perova all always made me feel welcome when I flew to Russia from the US. Lastly, while I still haven't met him in person, Jon Slaght has become a friend and mentor these last four years, helping me navigate the challenges with international research. To all of you, thank you so much for your support and friendship, and I look forward to many more years together!

Next, I would like to thank the Sikhote-Alin Biosphere Zapovednik for their support of this project. Svetlana Soutyrina, the director of the Zapovednik, has shown me constant kindness

and support over the years. Thank you for believing in this project. Kolya Reebin deserves special thanks for his help deploying our off-road cameras over the years. His knowledge of the Zapovednik was essential as we planned both camera deployments and snow track surveys. Anya Mukhachova helped me understand and process data from our FMP surveys, and is a great friend. All staff members of the Zapovednik have been kind and helpful with my Russian, and I thank you all for welcoming me into your world.

I would also like to thank Karann Putrevu, Ilya Khramulev, Lyesha Mogilyev, and Anzhelika Mogilyeva. Both Karann and Lyesha stepped up and helped deploy some of the most challenging random cameras in this project. Your friendship during my times in Terney made a world of difference for me. Whether through sharing music or adventuring out in freezing weather, our time together helped Terney feel like home. Lyesha Krutikov also helped with camera deployments during our first 2019-20 season. My thanks to all of you.

Lastly in Russia, I would like to thank the people who participated in our winter track surveys. It was a huge effort and many of the routes were challenging. Thank you for your hard work and especially for your patience as weather conditions continuously changed and we had to reschedule. Your efforts were an essential part of this project.

Back in Montana, I would like to thank all members – past and present – of the Hebblewhite and Brodie labs. Thank you for your friendship and support these last three years, especially during the COVID-19 pandemic. Our zoom-coffees and zoom-beers really made a difference. I look forward to the years ahead of friendship and collaboration. I also would like to thank the lab of Tom Martin. They offered me lab space my first semester, and quickly became a key support group as I struggled through my first semester. Thank you for your support.

Several individuals have been especially helpful these past three years with my data processing and analysis. Anna Moeller and Nick DeCesare provided fruitful conversations about the issue with measuring camera viewsheds, and it has been a pleasure collaborating with them on this topic. I would also like to thank Paul Lukacs for helping me understand the statistical models I used here, and for the valuable insights and interpretations of my results. Elie Gurarie helped me interpret GPS data and provided many insights about working in Russia. Kevin Morelle offered both guidance and an open door into the wonderful EuroBoar community. Arnaud Lyet and Tom Gray with WWF provided many useful discussions about applying the Space-To-Event model to motion-trigger data and have given me with several opportunities to present my work internationally, for which I am grateful.

I want to thank my wildlife biology family – Andrea Easter-Pilcher and Brian Pilcher, Pat Tucker and Bruce Weide, and the many biologist friends of my parents whom I'm proud to call my friends, too. Thanks to you, I knew that I could turn my passion for conservation into a career. You have all been wonderful role models over the years. I hope in my career that I stay as dedicated and passionate as you all have. Thank you for your inspiration.

I want to give a special thanks to my friends who came and visited me in Missoula over the years: Matt Floyd, Nick Milazzo and Mariah Dawson, Aidan McLaughlin, Will Muir, Tom Rahr, among others, and especially Helena Milazzo. I know I had an easier sell than most (Montana is the last best place!), but still, thank you for coming out and supporting me.

Lastly, I want to thank my family: my parents, Amy and John Waller, and my sister, Linda Waller. Both Amy and John are wildlife biologists and alumni of the University of Montana wildlife program. Graduating from the same program as you really is special. I am so proud to have role models in wildlife biology like you as my parents, too. Linda lived in Missoula during

my first two years of study, and since she is my best friend, made that time wonderful. Thank you for your unconditional love and support.

There are many others who over the last three years have supported me in this project. Though I haven't listed them by name, they were an integral part of my graduate experience and this project would not have come to fruition without their help. Thank you.

Because this thesis was only possible thanks to the many collaborations and shared efforts among many people, I will use "we" instead of "I" in the rest of this thesis.

CHAPTER 1: CAMERAS OR *CAMUS**? COMPARING CAMERA TRAPS AND SNOW TRACK SURVEYS TO ESTIMATE DENSITIES OF LARGE UNGULATE PREY

**Camus* (Russian: камус) refers to the skins Russian hunters attach to the bottoms of skis for traction in the snow.

1 | INTRODUCTION

For centuries, Large carnivore populations have suffered from the intensive and widespread anthropogenic threats of poaching, habitat loss and fragmentation, and prey depletion (Ripple et al. 2014). The loss of primary prey species through overhunting and poaching can decrease carnivore survival and recruitment (Fuller and Sievert 2001, Miquelle et al. 2010), increase human-carnivore conflicts (Graham et al. 2005, Miquelle et al. 2009, Lubis et al. 2020), and limit conservation efforts to restore carnivore populations (Aryal et al. 2016, Qi et al. 2021). Conservationists often cite prey recovery as an essential step towards halting the decline of predator populations (Wolf and Ripple 2016, Duangchantrasiri et al. 2016). Estimates of prey density are invaluable to these efforts, as they allow managers to document that recovery (Harihar et al. 2020), as well as to better understand the relationships between carnivores and their prey (Miquelle et al. 2010, Vinks et al. 2021).

The sustainable management of large herbivore prey species is essential for the recovery and persistence of wild tigers (*Panthera tigris*) across their range (Walston et al. 2010, Wikramanayake et al. 2011). Along with poaching of tigers and habitat loss, prey depletion has been identified as a major contributing factor to the collapse of tiger populations across Asia (Tilson et al. 1997, Dinerstein et al. 2007, Piper et al. 2008, Wolf and Ripple 2017). During the 2010 Global Tiger Summit, all 13 tiger range countries committed to recovering, sustainably managing, and monitoring prey populations to support tigers (Global Tiger Initiative 2010). But prey monitoring has proven difficult to implement. While guidelines exist that apply to some ecosystems where visibility of prey is high (Karanth and Nichols 2002), a decade after signing the

Global Tiger Initiative, most tiger range countries still do not have established systems for monitoring prey. There remains an urgent need to develop reliable and practical prey monitoring programs across tiger range.

In the Russian Far East, the importance of monitoring prey for Amur tiger (*P.t. altaica*) conservation has over twenty years of scientific support. Several studies have demonstrated how tigers select for areas of greater relative prey densities more than any landscape feature or vegetation (Miquelle et al. 1999, Hebblewhite and Mitchell 2013, Hebblewhite et al. 2014). Moreover, across their range, tigers appear to have a numerical response to increases in preferred prey densities (Karanth et al. 2004, Miquelle et al. 2010). In Russia, tigers occur at their lowest densities and low prey biomass is a major limiting resource (Miquelle et al. 2010). Estimates of prey densities will therefore help managers assess and maintain sufficient prey abundance to sustain tigers (Karanth and Nichols 2002, Hebblewhite et al. 2014, Jornburom et al. 2020).

Estimating the density of large herbivore prey has proven challenging across ecosystems and management contexts. Individuals of most large herbivores cannot be uniquely identified, precluding the application of capture-recapture models as used to monitor tiger densities (Karanth 1995, Karanth and Nichols 2002, Efford et al. 2009, Royle et al. 2009). In places such as India, where animal visibility is high, prey densities are also high, and animals tend not to flee from humans, distance sampling offers a reliable approach to precisely estimate herbivore densities (Karanth and Nichols 2002, Harihar et al. 2014, Jhala et al. 2020, Karanth et al. 2020). However, many ecosystems do not share these attributes. Limited visibility due to topography or vegetation and low densities of hunted, wary prey require managers to survey using other methods. In Russia, wildlife managers use a snow-tracking method called the Formozov-Malyushev-Pereleshin (FMP) method to track prey densities (Formozov 1932, Chelintsev 1995, Lomanov

2000, Stephens et al. 2006b) see methods and Table 1-1). The FMP method provides valuable long-term datasets across Russia and has been recently validated in the Western literature (Stephens et al. 2006b, Keeping et al. 2018, Ahlswede et al. 2019). However, the FMP method requires considerable survey effort, is prone to bias caused by convenience sampling, and when applied using snow track surveys, depends on consistent, recurring snowfall. The dependence on snowfall has become a major concern in the Russian Far East with climate change leading to warming temperatures that make tracking conditions more challenging (Stephens et al. 2006a, IPCC 2022). These drawbacks compromise the FMP method's dependability as a future survey method in the Russian Far East. This has important consequences considering the number of publications that use prey density estimates from the FMP to inform Amur tiger conservation (Miquelle et al. 1999, 2005, 2010, Petrunenko et al. 2016, Jiayin et al. 2018, Qi et al. 2021). Russian wildlife managers, like many large carnivore and ungulate managers world-wide, need alternative methods to monitor herbivore prey species.

Camera traps ('cameras' hereafter) offer a promising solution to this problem since many researchers are already using cameras to monitor large carnivores such as tigers. For example, Kafley et al. (2019) recently applied *N*-mixture models (Royle et al. 2004) to estimate tiger prey abundance in Chitwan National Park, Nepal, using "by-catch" photos of prey obtained while surveying tigers. Xiao et al. (2018) similarly used cameras placed for tiger monitoring to estimate prey abundance with *N*-mixture models on the Hunchun Nature Reserve in northeast China. Tempa (2017) also applied *N*-mixture models to evaluate the effects of relative prey abundance on tiger occupancy across Bhutan. While the estimates of relative prey abundance and inclusion of spatial covariates in these studies provided inference about variation in relative prey densities, they measure relative or local abundance (i.e., the number of individuals occurring in the vicinity

of a particular camera trap) rather than densities of prey at the landscape scale. *N*-mixture models also make challenging assumptions about detections and animal movements, particularly for social species such as many ungulates. To meet these assumptions, cameras must be placed according to the home range size of the study species, which is a problem for multi-species monitoring with the same cameras. These requirements ultimately limit *N*-mixture models' ability to track trends in prey abundance (Kery and Royle 2015).

Several alternative models have been proposed in the last 15 years that estimate densities of unmarked populations by extrapolating density within the collective sampled areas in front of cameras ("viewsheds") (Gilbert et al. 2020). These include the Random Encounter Model (REM) (Rowcliffe et al. 2008), the Random Encounter and Staying Time model (REST) (Nakashima et al. 2018), Camera Trap Distance Sampling (CT-DS) (Howe et al. 2017), and the Space-To-Event and Time-To-Event models (STE and TTE) (Moeller et al. 2018). These models (collectively, "viewshed density estimators") have been used to estimate densities of both carnivores (Cusack et al. 2015, Doran-myers et al. 2021, Loonam et al. 2021, Ausband et al. 2022) and herbivore prey species (Rowcliffe et al. 2008, Moeller et al. 2018, Morelle et al. 2020, Palencia et al. 2021) across diverse ecosystems. While the number of tests and validations of these models are growing, they are still relatively new and make some common, challenging assumptions about sampling designs and statistical analyses (Table 1-1) that may limit their feasibility for monitoring tiger prey. For instance, viewshed density estimators assume that (1) animals move independent of the camera viewsheds, and (2) that these viewsheds are representative of the physical characteristics of the study area that likely affect both animal movement and density. This requires researchers to implement some form of randomized or systematic sampling design, which translates to much greater effort than setting up cameras on roads and trails for tiger

density monitoring (see Chapter 2 of this thesis). Most of the published estimates of these models also had poor precision, and the large number of cameras needed to achieve desired precision may be prohibitive (Morin et al. 2022). Moreover, none of these models have been published as a reliable and practical means to monitor densities of prey for tiger conservation.

To address this question of whether cameras can be used to monitor prey of tigers, we deployed cameras under a systematic random sampling design over two winters (2019-20 and 2020-21) to estimate densities of the four main prey species of the Amur tiger in the Russian Far East (Miquelle et al. 1996, 2010, Kerley et al. 2015): wild boar (*Sus scrofa ussuricus*), red deer (*Cervus canadensis* ssp. *xanthopygus*), roe deer (*Capreolus pygargus*), and sika deer (*Cervus nippon*). First, we conducted winter track surveys using both conventional and representative survey designs to estimate prey densities using the FMP method. We then compared these to estimates from three viewshed density estimators: the REM, STE, and TTE models. Finally, we followed Riley et al. (2017) and evaluated the statistical, logistical, and cost considerations of each model. As an important part of this assessment, we simulated the number of cameras needed to achieve a 20% coefficient of variation (CV) for different levels of prey densities in our study area (a goal set for this study area by Stephens et al. (2006b)). This allowed us to thoroughly evaluate each estimator's potential to monitor prey in the Russian Far East.

2 | MATERIALS AND METHODS

2.1 Study Area

This study took place in the 4,016 km^2 Sikhote-Alin Biosphere Zapovednik ("Zapovednik"), Primorskyi Krai, Russia. Zapovedniks are a unique type of nature preserve in which entry is restricted to only Zapovednik staff and permitted researchers. The Sikhote-Alin Biosphere Zapovednik is named after the Sikhote-Alin Mountains, a low-elevation range running northeast

through the preserve. Summers in the Zapovednik are hot and wet, while winters are relatively cold and dry. The reserve is mostly forested, with coastal Mongolian oak (*Quercus mongolica*) and mixed hardwood forests transitioning to mixed forests of Korean pine (*Pinus koreansis*) further inland. These forest transitions result in important spatial variation in mast crop availability for wildlife, as acorns and pine nuts are dominant sources of food for much of the community (Heptner et al. 1988). Our study took place in a 527 km^2 area within the Zapovednik and south of the Dalnyi range, which separates the Serebryanka river basin to the north from the Golubichnoe and Djigitovka drainages to the south (Figure 1-1).

The ungulate community in our study area is made up of six species: the four main prey species mentioned above, along with the smaller and rarer goral *(Naemorhedus caudatus*) and musk deer (*Moschus moschiferus*). Sika deer are only common along the coast of the Zapovednik, though their range is expanding and they seem to exclude red deer (Stephens et al. 2006a). Amur tigers are the dominant predator in the community, often excluding wolves (*Canis lupus*) from their territory (Miquelle et al. 2005). Brown bears (*Ursus arctos*) and Himalayan black bears (*Ursus thibetanus*) forage on the same mast crops as ungulates, and tigers will sometimes prey on these bear species as well (Miquelle et al. 1996).

2.2 Formozov-Malyushev-Pereleshin (FMP) density estimation

The FMP method has been the standard for wildlife surveys throughout Russia for decades, including our study area (Formozov 1932, Chelintsev 1995, Lomanov 2000, Stephens et al. 2006a). The FMP method estimates density by relating the encounter rate of fresh (<24h old) tracks observed along walked/skied transects with independent estimates of the study species' daily travel distance. In the FMP formula, the density *D* of a population is estimated by:

$$D = \frac{\pi}{2}\frac{x}{S\,\widehat{M}} \quad \text{(Equation 1)}$$

Where x is the total number of tracks encountered, S is the total length of all transects, and $\widehat{M}$ is the study species' daily travel distance. The term $\frac{\pi}{2}$ relates the species' daily travel distance to the probability of encountering a track along the surveyed transects, integrated over all possible angles of intersection between animal's movement paths and the transects (Stephens et al. 2006b). The FMP method assumes: (1) geographic and demographic closure; (2) the age of species' tracks is identified without error; (3) animals move independent of transects; and (4) transects are representative of the study area (Table 1-1). Historically, the Zapovednik has conducted surveys only along roads and trails due to limitations of staff and resources. However, this is a violation of assumptions (3) and (4) above (Stephens et al. 2006a). We therefore estimated density of prey species first with the conventional survey routes along roads and trails ("conventional surveys"), and second, with survey routes representative of the study area and independent of animal movement ("random surveys"). These random surveys were not laid out in a truly random fashion but were designed to be distributed across the entire study area, accessible, and representative of the slopes, elevations, and aspects of the study area. Random surveys were conducted as close in time to the conventional surveys as possible (Table 1-2).

For each survey, teams of two surveyors walked, skied, or snowmobiled transects and recorded the number of fresh tracks of wild boar, red deer, roe deer, and sika deer. All tracks (including re-crossings of the same individual) were counted (Keeping and Pelletier 2014). To inform the daily travel distance parameter, we used estimates and associated error from Stephens et al. (2006a) for the three deer species. For wild boar, we estimated daily travel distance and variance by analyzing fine-scale (15-minute fixes) GPS relocation data from collared wild boar in the same study area (Appendix 1B). We used nonparametric bootstrapping (Efron and Tibshirani

1993) to estimate 95% confidence intervals of each density estimate. First, encounter rates (x/S) were sampled with replacement 5,000 times from the data, along with a daily travel distance (M) drawn from values reported by Stephens et al. (2006a) and our wild boar estimates. These parameter values were used for 5,000 estimates of density from which final 95% confidence intervals and coefficients of variation (CVs) were generated (Efron and Tibshirani 1993, Stephens et al. 2006b).

2.3 Random Encounter Model (REM)

The REM was first proposed by Rowcliffe et al. (2008) to estimate the density of wildlife populations using cameras for species whose individuals cannot be uniquely identified. The REM was derived from both ideal gas theory (Hutchinson and Waser 2007) to describe animal movements and from the FMP formula (Stephens et al. 2006b) to relate animal movement to the probability of being detected by cameras. Rowcliffe et al. (2008) derived the following equation to estimate density *D:*

$$D = \frac{y}{t}\frac{\pi}{vr(2+\theta)} \quad \text{(Equation 2)}$$

Where *y* is the number of independent detections of the individuals, *v* is the average daily travel distance of the animal, *t* is the total number of days that cameras were deployed, and *r* and θ are the average radius and angle of the sampled area in front of the cameras. The REM uses the sampled area in front of cameras both as a component of survey effort, as well as to relate the study species' speed to the probability of being detected within a camera's sampled area. If surveys are conducted on a line and theta (θ) is therefore zero, and if the radius of the camera (*r*) is replaced by the total length of all transects (*S* in Equation 1), then Equation 2 matches exactly the FMP formula (Rowcliffe et al. 2008). The assumptions of the REM are similar to those of the

FMP: (1) geographic and demographic closure; (2) the ideal gas model accurately describes the movement of the study species and results in a Poisson distribution of animals across the study area (Hutchinson and Waser 2007); (3) detections *y* of animals are independent; (4) animals move independently of camera traps; and (5) cameras are representative of the study frame (Table 1-1).

We considered detections of individuals of the same species 30-minutes apart to be independent. Speed estimates were derived as for the FMP. We used 5,000 iterations of non-parametric bootstrapping of both the encounter rate $\frac{y_i}{t_i}$ of each camera *i,* and the daily travel distance *v* to generate a bootstrapped distribution of density estimates. This distribution gave us point estimates of density, 95% confidence intervals, and coefficients of variation.

2.4 Space-To-Event (STE) Model

Rather than using the number of independent detections of animals as a parameter in the estimator, the Space-To-Event (STE) model makes use of the relationship between the exponential and Poisson distributions to estimate their shared rate parameter, lambda (λ), which is the average number of animals per unit area. If animals are assumed to be Poisson-distributed across the study area, then the amount of sampled area, *S,* until a detection will be exponentially distributed (Moeller et al. 2018):

$$S \sim Exp(\lambda) \quad \text{(Equation 3)}$$

The sampled areas in front of the cameras are selected in random order until a detection (i.e., "Space-To-Event") at regular intervals of time ("occasions"). With many occasions, these observed spaces-to-event form an exponential distribution from which lambda and associated variance are estimated by maximum likelihood estimation. If there are no animal detections at any camera during an occasion, then that occasion is right-censored. So long as these measurements of space-to-event are instantaneous in time, the STE model estimates density independent of

animal movement rate. The STE model also does not require counts or independent estimates of group size given the time-to-event framework of the estimator (Moeller et al. 2018, Moeller and Lukacs 2021). The STE model assumes: (1) geographic and demographic closure; (2) detections of animals at occasions are independent; (3) animals are Poisson-distributed across the cameras' sampled areas; (4) animals move independently of camera traps; and (5) cameras are representative of the study area.

The STE was initially designed to estimate density using time-lapse photography (Moeller et al. 2018). However, because of our expected low densities of prey, our camera data was collected using motion-trigger photography, which meant there were times when an animal was present in front of a camera, but not detected. We therefore estimated the average number of seconds between images where the animal was most likely to still be in front of the camera (following Becker et al. 2021), then used this as our sampling window. If this still resulted in zero detections across the spaces-to-event, we then increased the window to 60 seconds (Table 1-3). We used 15-minute occasions to balance precision and the assumption of independence of each measured space-to-event. The approach we used to determine the sampling window violates the assumption of instantaneous sampling (Moeller et al. 2018), but was necessary to obtain at least one detection used in the measured spaces-to-event to estimate density. To better understand the consequences of increasing the sampling window length, we next estimated densities with increasing sampling window lengths (1-60 seconds) and occasion lengths (1.5, 5, 10, and 15 minutes). Variances in the density estimates were produced using the delta method, from which we obtained 95% confidence intervals and coefficients of variation.

2.5 Time-To-Event (TTE) Model

The concept of the TTE model is like the STE model, relying on the same Poisson-exponential relationship to estimate lambda. Instead of instantaneously sampling across all cameras in the study area on each occasion, the TTE model samples space at each individual camera during shorter, regular intervals of time ("periods") within each occasion. If the length of these periods is only long enough for animals to cross the viewshed of the camera, then the number of periods (i.e., the amount of sampled space at one camera across time) until a detection will be exponentially distributed (Moeller et al. 2018):

$$T \sim Exp(\lambda) \quad \text{(Equation 4)}$$

Lambda, the average number of animals in a camera's sampled area, is estimated with the exponential likelihood from the observed times-to-event of the species of interest at each camera. The TTE model makes the same assumptions as the STE model: (1) geographic and demographic closure; (2) detections of animals in each occasion are independent; (3) animals are Poisson-distributed across the cameras' viewsheds; (4) animals move independently of camera traps; (5) cameras are representative of the study area. Unlike the STE model, the TTE requires estimates of animal movement rate to determine the period length.

2.6 Camera trap study design

The REM, STE and TTE models all share the assumptions that animals move independently of cameras and that cameras are representative of the study area. To best meet these assumptions, we used a systematic random sampling design for camera locations (Figure 1-1). First, a rectangular 3.5 × 3.5 km grid was drawn over our study area. This cell size is roughly the average area of a female red deer's home range (Dou et al. 2019). We randomly generated one camera location in each cell, then excluded cameras that were not within the bounds of our study area. This allowed us to objectively include or exclude cameras in cells that were only partially included in the study

area. Different locations were generated for the 2019-20 and 2020-21 winter seasons. Because of the remoteness of much of the western part of the area, a few cameras' locations were adjusted to be more easily accessed, while maintaining the random location's forest type, elevation, and aspect.

Cameras were deployed as close to the randomly generated coordinate as possible, while also selecting camera sites that would have minimal obstructions (e.g., dense shrubs, cliffs, dense trees) within the cameras' viewsheds. Because of resource constraints, whenever cameras used for monitoring tigers by the Zapovednik were inside a grid cell, we placed a camera roughly 150 m away from that tiger camera and considered that camera as the random camera for that cell (see Chapter 2). Cameras were placed 1 – 1.5 m above the ground, facing north to minimize glare from the sun, and were active 24 hours per day. Whenever the camera site was on a slope, the camera was positioned such that its horizontal field of view was in-line with the slope to minimize reductions in detection area (Moeller et al. 2018; Appendix 1A, Figure A3). Camera settings were configured to take bursts of three photos at each capture with no delay to best approximate continuous sampling. No baits or lures were used.

All camera density estimators require measurements of the camera viewshed to extrapolate detections to space. In this study, we used two different measurement techniques to measure camera sampled area (Appendix 1A). For winter 2019-20, we performed extensive walk tests to determine detection distance and angle of each camera. In winter 2020-21, we measured the viewable area in front of each camera, constrained by the maximum detection distance.

2.7 Methods comparison

To fully assess the potential of the above estimators for monitoring tiger prey, we developed a ranking system following Riley et al. (2017) based on i) statistical, ii) logistical, and iii) cost

categories. For each of these three categories, we developed criteria to compare either each estimator or each class of estimator. Each criterion was developed to score estimators relative to one another, with 1 being the best score and 4 being the worst. A brief description of each criterion is provided in Table 1-3, and the details of how we scored each estimator for each criterion are provided in Appendix 1C.

2.8 Data processing and analysis

Estimates of density were performed using the R programming language in R Studio (R Core Team 2022). After we classified camera trap images, we converted them to detection data in R using the *camtrapR* package (Neidballa et al. 2016). To determine our study period, we chose a 60-day window when detections of each prey species were most consistent over time, and thus best met the assumptions of the viewshed density estimators. We adapted previously developed R code for REM and FMP density estimates. For STE and TTE estimates, we used the *spaceNtime* package (Moeller and Lukacs 2021).

3 | RESULTS

3.1 Surveys

We conducted 103 km of conventional winter track surveys in winter 2019-20 and 117 km of surveys during the winter 2020-21. We conducted 64 km of random track surveys in winter 2019-20 (Figure 1-1). However, because of the COVID-19 pandemic, we were unable to conduct random surveys in winter 2020-21. Thus, the comparison of conventional and random survey routes was only possible during winter 2019-20.

We deployed 50 camera traps in winter 2019-20 and 57 cameras in winter 2020-21. Five cameras malfunctioned in winter 2019-20, and seven malfunctioned in winter 2020-21, resulting

in data from 45 cameras (2,743 trap nights across 60 days, February 01, 2020 to April 01, 2020) and 50 cameras (3,098 trap nights across 60 days: December 10, 2020 to February 10, 2021), respectfully (Table 1-2; Figure 1-1). We used a variety of camera brands and models in winter 2019-20, but only two models during winter 2020-21 (Table 1-2).

3.2 Prey density estimates

We developed a total of 36 estimates of density across species, years, and methods (Figure 1-2, Table 1-4). Across all estimators, STE and FMP estimates from random surveys were the most similar during 2019-20 (Figure 1-2). Among viewshed density estimators, the STE and REM were more similar than the TTE. Conventional snow track surveys estimated higher densities than the random surveys in 2019-20, but to varying degrees for each species.

Precision varied among species and estimators (Figure 1-2; Table 1-4). The TTE was the most precise for all species and across seasons (average coefficient of variation 21%). The STE estimated relatively low coefficients of variation (average 29%) for high-density species such as wild boar in 2019-20 but had the largest values for low-density species like roe deer and wild boar in 2020-21 (average CV of 99%). The conventional snow track surveys estimated slightly better average precision than the random surveys (average coefficient of variation 39% vs. 47% in winter 2019-20), though wild boar and sika deer estimates were considerably more precise for random surveys (Figure 1-2).

3.3 Methods comparison

In our assessment of the statistical, logistical, and cost constraints of each estimator, FMP surveys consistently scored better than the viewshed density estimators (Table 1-5). We only included random FMP surveys in the comparison because of the bias we found in conventional surveys

(Figure 1-2). The FMP scored well because it was a simple model to implement and did not require any specialty equipment (i.e., cameras). The FMP's weakest score was in logistics, as planning for FMP surveys was dependent on appropriate snow and weather conditions.

Among camera-based estimators, the STE and TTE scored identically. The STE scores were reduced because it did not require independent estimates of movement, which can be costly to derive. While the TTE had more sources of bias and required estimates of animal movement, it was considerably more precise than the other estimators. This meant that less cameras were necessary to achieve the desired 20% coefficient of variation, which reduced start-up costs and time spent processing and analyzing data. Even so, start-up costs to achieve 20% CV for medium-density populations (0.7 km^{-2}) were high for all camera estimators, with $16,920 being the cheapest cost for the TTE. The STE, which scored better in other categories, would require $27,020 to purchase 120 cameras, memory cards, and sufficient batteries (Table 1-5).

4 | DISCUSSION

Prey depletion remains a pressing global threat faced by carnivores (Wolf and Ripple 2016). As conservationists work to recover prey populations, estimates of prey densities are an invaluable metric to assess the success of conservation actions (Williams et al. 2002, Nichols and Williams 2006, Karanth et al. 2017). To test whether camera traps offer a viable tool to monitor densities of ungulate prey in the Russian Far East, we applied the REM, STE, and TTE viewshed density estimators and compared them with independent estimates from the FMP snow tracking method. Estimates from the STE and FMP estimates from random surveys provided consistently similar results across species during the 2019-20 winter (Figure 1-3). The STE was also consistent across years for all species except for wild boar, as expected (Figure 1-3; discussed below). Other authors have found support for the STE for other species such as large herbivores (Moeller et al.

2018) and carnivores (Loonam et al. 2021, Ausband et al. 2022) in Idaho, USA. Among viewshed density estimators, the STE also scored well compared to other camera-based estimators according to our rubric (Table 1-5), largely because it does not require an estimate of animal movement (Appendix 1C). These results provide the most support for the STE model.

Despite the consistency between the STE and FMP, there are challenges when applying the STE to motion-trigger data. STE estimates are sensitive to the chosen sampling window length (Figure 1-4; Loonam et al. 2021a), and it remains unclear how best to choose a specific sampling window length when analyzing motion-trigger data. Motion-trigger cameras do not perfectly detect all animals that pass through their detection zone at every second, as we saw in our own data. This translates to non-continuous sampling of the collective camera viewsheds, and therefore occasions when there really is an animal within a viewshed when estimating space-to-event, but no image of that animal at that exact second. When we used a one-second sampling window, density estimates were very low or simply not estimable because there were no detections (Figure 1-4). This was a result of both the low density of that population and the negative bias caused by non-continuous sampling. Increasing the sampling window eventually provided a detection with which to measure space-to-event. Both Loonam et al. (2021a) and Ausband et al. (2022) also increased their sampling windows beyond one second, but it is unclear why they chose their respective sampling window lengths. When we used the average number of seconds between frames of the same capture sequence as our sampling window, following Becker et al. (2022)'s technique, we obtained at least one detection for only three of our eight STE estimates (Table 1-3). We then used a 60-second sampling window and obtained estimates, but this decision was arbitrary and violated the assumption of instantaneous sampling (Moeller et al. 2018). This sampling window and non-continuous sampling issue suggests three conclusions

about the STE. First, if possible, managers should use time-lapse photography when applying the STE to avoid the issues caused by imperfect detection (Moeller and Lukacs 2021). This will only be possible if the cameras have time-lapse capabilities, if the study species is at a sufficiently high density, and/or if the managers have enough cameras to obtain at least one detection. Second, the STE may only be reasonably applied to animal populations of sufficiently high density. At a certain low population density, the STE is simply not estimable without increasing the sampling window length by an arbitrary amount, which compromises the reliability of the estimate. Third, if researchers use motion-trigger data, they should be cautious when applying the STE. Detection data should be examined to determine how frequently instances occur where an animal is likely within the viewshed but not detected by cameras. Our adopted approach from Becker et al. (2022) provides a reasonable way to choose a sampling window length, but only if there are sufficient detections. More work is needed to determine how best to apply the STE to motion-trigger data, and the authors are collaborating with other researchers on this challenge.

An additional challenge with the STE is its relatively poor precision. If Russian wildlife managers wish to achieve at least 20% CV in annual estimates of density using the STE, our simulations indicated that they would need to deploy considerably more cameras than we did in this study (Figure 1-3). For most conservation programs in Russia and across tiger range, resource and time constraints make this precision goal in annual estimates infeasible for all except the highest prey population densities. When auxiliary movement data is available, the TTE provides an alternative model with relatively high precision (Table 1-5). However, we found estimates were consistently higher than other estimates (Figure 1-2). Santini et al. (2022) also found the TTE to overestimate densities when tested against more realistic simulations of animal movement. The TTE is more precise than other viewshed density estimators largely because of its

stricter assumptions about animal movement, rooted in the static period length used to estimate time-to-event. Because the movements of our study species are variable during the winter (Stephens et al. 2006b; Appendix 1B), the inflexibility of the period length in the TTE in its current form was likely the cause of bias in our estimates.

Camera-based approaches are limited by start-up costs, demands for field staff, and the image processing necessary to the desired level of precision in our study area. This limits the applicability of such approaches to organizations with substantial resources. In contrast, the FMP model provided levels of precision similar to the camera-based estimators at much lower cost. This is consistent with Keeping et al.'s (2018) findings that FMP surveys in the Kalahari desert offered a cost-effective alternative to aerial surveys for community-level monitoring. However, when tracks are recorded in snow, the logistics of planning sufficient surveys in a short period of time (i.e., when tracks are still present and identifiable) are a major limitation. In our case, we had to re-schedule surveys multiple times because of changing snow conditions. Moreover, while linear trends since 1966 suggest the Russian Far East may see increased snow precipitation in the coming decades (Bulygina et al. 2011), the latest predictions in the sixth assessment report by the Intergovernmental Panel on Climate Change clearly indicate significant warming in this region in the near future (IPCC 2022). Even if there is more snow precipitation in the Far East, these warming temperatures will make snow conditions challenging for accurately identifying track age. Still, the FMP method is statistically well-supported (Stephens et al. 2006b, Jousimo and Ovaskainen 2016, Keeping et al. 2018), and FMP density estimates were consistent with viewshed density estimators generally (Figure 1-2).

Our results support the FMP method as a reliable tool to monitor densities of unmarked wildlife populations for researchers and managers with limited resources and in snow-covered

environments. But this is only if the assumption of representative sampling of the landscape is met. Our FMP estimates from surveys along roads and trails were consistently higher than our representative surveys (Figure 1-2). These roads and trails were typically along rivers and creeks and avoided high elevations with more snow. Hebblewhite et al. (2014) found all four prey species selected habitats with the same characteristics as these roads and trails at the scale of second-order selection (Johnson 1980). At finer scales, prey species may select the roads and trails themselves for their ease of travel. For instance, herds of sika deer seem to prefer using established game trails to travel in the winter (Zapovednik staff, pers comm). This behavior led to greater track counts and therefore higher density estimates. Conducting representative surveys is arduous work, but we strongly recommend this as an essential part of study design if density estimates are to be an unbiased representation of the entire study area.

Many researchers do not work in snow-covered environments, and as such are still searching for camera-based solutions to unmarked population monitoring. All viewshed density estimators are limited by the strict assumption of random sampling and need for a large number of cameras to achieve better precision. There are two important areas of development that could improve the precision of the STE and all other camera-based estimators. First, repeated estimates over time can be used to increase overall precision in population trend. Integrated population models (IPMs) combine abundance or count data over time with other sources of information on demographic parameters to improve the precision of estimates (Schaub et al. 2007, Schaub and Abadi 2011). The inclusion of spatial covariates could improve the precision of density estimates as well. For example, Allen et al. (2008) found that by stratifying aerial surveys according to different bins from resource selection function models, they improved both precision of elk (*Cervus canadensis*) abundance estimates and design efficiency. In our case, we struggled to

obtain precise estimates for sika deer, both in our real data (Table 1-4) and simulation extensions. Sika deer are mostly concentrated near the coast in our study area, so our detection data varied considerably across the whole study area. A simple categorical covariate for coastal oak would explain a lot of the variation in our detections of sika deer across cameras and therefore improve the precision of density estimates.

Even with poor precision, we demonstrated that the estimators tested here are all capable of detecting dramatic changes in abundance. We detected a 95% decline (averaged across estimators) in wild boar densities (Figure 1-2), even though CVs of estimates in winter 2020-21 were over 100% for some models (Table 1-4). Our study was concurrent with the arrival of African Swine Fever (ASF) in our study area in 2020 (Zakharova et al. 2021), so this decline was not surprising. These are the first estimates of the population-level consequences of ASF infection in Russia. This level of decline aligns well with that observed by Morelle et al. (2020), who detected a 95% decline in wild boar densities in two forests in and near Biolowiecza Primordial Forest, Poland. Our estimates can be used as a reference when wildlife managers consider the consequences of ASF spread into currently uninfected populations.

5 | CONCLUSION

Twelve years after the World Tiger Summit, and with the second summit planned for this year, most countries still have not established reliable prey monitoring programs. Here, we tested three viewshed density estimators against independent estimates from snow track surveys and assessed each estimator's potential to serve as a tool for monitoring densities of large herbivore prey. While precision was generally poor, estimates of densities were mostly consistent and, importantly, all estimators detected a real, dramatic decline in wild boar densities. The consistency of estimates both over time and with our random snow track surveys suggest that

these models can provide unbiased estimates of density. With more development, such as the inclusion of spatial covariates and consistent monitoring over time, the precision of density estimates can be improved. Even so, the strict assumptions of all models that cameras representatively sample the study area remain restrictive. This is especially challenging because of the rugged terrain in much of tiger habitat and low densities of wary prey. In the next chapter, we assessed the importance of this assumption by comparing detections of ungulate prey at cameras placed randomly or on roads. We also tested an alternative deployment strategy that aimed to balance the need for random sampling with its logistical constraints.

6 | LITERATURE CITED

Ahlswede, S., E. C. Fabiano, D. Keeping, and K. Birkhofer. 2019. Using the Formozov–Malyshev–Pereleshin formula to convert mammal spoor counts into density estimates for long-term community-level monitoring. African Journal of Ecology 57:177–189.

Allen, J. R., L. E. Mcinenly, E. H. Merrill, and M. S. Boyce. 2008. Using Resource Selection Functions to Improve Estimation of Elk Population Numbers. Journal of Wildlife Management 72:1798–1804.

Aryal, A., R. P. Lamsal, W. Ji, and D. Raubenheimer. 2016. Are there sufficient prey and protected areas in Nepal to sustain an increasing tiger population? Ethology Ecology and Evolution 28:117–120.

Ausband, D. E., P. M. Lukacs, M. Hurley, S. Roberts, K. Strickfaden, and A. K. Moeller. 2022. Estimating wolf abundance from cameras. Ecosphere 13.

Bulygina, O. N., P. Y. Groisman, V. N. Razuvaev, and N. N. Korshunova. 2011. Changes in snow cover characteristics over Northern Eurasia since 1966. Environmental Research Letters 6.

Chauvenet, A. L. M., R. M. A. Gill, G. C. Smith, A. I. Ward, and G. Massei. 2017. Quantifying the bias in density estimated from distance sampling and camera trapping of unmarked individuals. Ecological Modelling 350:79–86.

Chelintsev, N. G. 1995. Mathematical principles of winter censuses of mammals. Byull. Mosk. Ova. Ispyt. Prir. 100:3–19.

Cusack, J. J., A. Swanson, T. Coulson, C. Packer, C. Carbone, A. J. Dickman, M. Kosmala, C. Lintott, and J. M. Rowcliffe. 2015. Applying a random encounter model to estimate lion density from camera traps in Serengeti National Park, Tanzania. Journal of Wildlife Management 79:1014–1021.

Dinerstein, E., C. Loucks, E. Wikramanayake, J. Ginsberg, E. Sanderson, J. Seidensticker, J. Forrest, G. Bryja, A. Heydlauff, S. Klenzendorf, P. Leimgruber, J. Mills, T. G. O'Brien, M. Shrestha, R. Simons, and M. Songer. 2007. The fate of wild tigers. BioScience 57:508–514.

Doran-myers, D., A. J. Kenney, C. J. Krebs, C. T. Lamb, A. K. Menzies, D. Murray, E. K. Studd, J. Whittington, and S. Boutin. 2021. Density estimates for Canada lynx vary among estimation methods.

Duangchantrasiri, S., M. Umponjan, S. Simcharoen, A. Pattanavibool, S. Chaiwattana, S. Maneerat, N. S. Kumar, D. Jathanna, A. Srivathsa, and K. U. Karanth. 2016. Dynamics of a low-density tiger population in Southeast Asia in the context of improved law enforcement. Conservation Biology 30:639–648.

Efford, M. G., D. L. Borchers, and A. E. Byrom. 2009. Density estimation by spatially explicit capture-recapture: likelihood-based methods. Modeling demographic processes in marked populations:255–269.

Efron, B., and R. J. Tibshirani. 1993. An introduction to the Bootstrap. Chapman & Hall, New York.

Formozov, A. N. 1932. Formula for quantitative censusing of mammals by tracks. Russ. J. Zool. 11:66–69.

Fuller, T. K., and P. R. Sievert. 2001. Carnivore demography and the consequences of changes in prey availability. Pages 163–178 *in* J. L. Gittleman, S. M. Funk, D. W. MacDonald, and R. K. Wayne, editors. Carnivore Conservation. Cambridge University Press.

Gilbert, N. A., J. D. J. Clare, J. L. Stenglein, and B. Zuckerberg. 2020, February 1. Abundance estimation of unmarked animals based on camera-trap data. Blackwell Publishing Inc.

Global Tiger Initiative. 2010. Global Tiger Recovery Program 2010–2022. Page Conference Document for Endorsement.

Graham, K., A. P. Beckerman, and S. Thirgood. 2005. Human-predator-prey conflicts: Ecological correlates, prey losses and patterns of management. Biological Conservation 122:159–171.

Gray, T. N. E. 2018. Monitoring tropical forest ungulates using camera-trap data. Journal of Zoology 305:173–179.

Harihar, A., B. Pandav, M. Ghosh-Harihar, and J. Goodrich. 2020. Demographic and ecological correlates of a recovering tiger (Panthera tigris) population: Lessons learnt from 13-years of monitoring. Biological Conservation 252.

Harihar, A., B. Pandav, and D. C. Macmillan. 2014. Identifying realistic recovery targets and conservation actions for tigers in a human-dominated landscape using spatially explicit densities of wild prey and their determinants. Diversity and Distributions 20:567–578.

Hebblewhite, M., D. G. Miquelle, H. Robinson, D. G. Pikunov, Y. M. Dunishenko, V. V. Aramilev, I. G. Nikolaev, G. P. Salkina, I. V. Seryodkin, V. V. Gaponov, M. N. Litvinov, A.

V. Kostyria, P. V. Fomenko, and A. A. Murzin. 2014. Including biotic interactions with ungulate prey and humans improves habitat conservation modeling for endangered Amur tigers in the Russian Far East. Biological Conservation 178:50–64.

Hebblewhite, M., and M. S. Mitchell. 2013. Carnivore habitat ecology: integrating theory and application. Pages 218–255 *in* L. Boitani and R. A. Powell, editors. Carnivore Ecology and Conservation: A Handbook of Techniques. Oxford Scholarship Online.

Heptner, V. G., A. A. Nasimovich, and A. G. Bannikov. 1988. Mammals of the Soviet Union: Volume 1. Smithsonian Institution, Washington D.C.

Howe, E. J., S. T. Buckland, M. L. Després-Einspenner, and H. S. Kühl. 2017. Distance sampling with camera traps. Methods in Ecology and Evolution 8:1558–1565.

Hutchinson, J. M. C., and P. M. Waser. 2007, August. Use, misuse and extensions of "ideal gas" models of animal encounter.

IPCC. 2022. Climate Change 2022: Impacts, Adaptation, and Vulnerability. Page (D. C. R. M. T. E. S. P. K. M. A. A. M. C. S. L. S. L. V. M. A. O. B. R. (eds.)] Contribution of Working Group II to the Sixth Assessment Report of the Intergovernmental Panel on Climate Change [H.-O. Pörtner, Ed.). Cambridge University Press.

Jhala, Y. V., Q. Qureshi, and A. K. Nayak. 2020. Status of tigers, copredators, & prey in India, 2018. New Dehli.

Jiayin, G. U., Y. U. Lan, Y. Hua, Y. Ning, B. Heng, Q. I. Jinzhe, Z. Long, M. Yao, C. Huang, L. I. Zhilin, J. Lang, G. Jiang, and M. A. Jianzhang. 2018. A comparison of food habits and prey preferences of Amur tiger (Panthera tigris altaica) at the southwest Primorskii Krai in Russia and Hunchun in China. Integrative Zoology 13:595–603.

Johnson, D.H. 1980. The Comparison of Usage and Availability Measurements for Evaluating Resource Preference. Ecology 61: 65-71.

Jornburom, P., S. Duangchantrasiri, S. Jinamoy, A. Pattanavibool, J. E. Hines, T. W. Arnold, J. Fieberg, and J. L. D. Smith. 2020. Habitat use by tiger prey in Thailand's Western Forest Complex: What will it take to fill a half-full tiger landscape? Journal for Nature Conservation 58.

Jousimo, J., and O. Ovaskainen. 2016. A spatioorally explicit random encounter model for large-scale population surveys. PLoS ONE 11.

Kafley, H., B. R. Lamichhane, R. Maharjan, B. Thapaliya, N. Bhattarai, M. Khadka, and M. E. Gompper. 2019. Estimating prey abundance and distribution from camera trap data using binomial mixture models. European Journal of Wildlife Research 65.

Karanth, K. U. 1995. Estimating tiger Panthera tigris populations from camera-trap data using capture-recapture models. Biological Conservation 71:333–338.

Karanth, K. U., N. S. Kumar, and K. K. Karanth. 2020. Tigers against the odds: Applying macro-ecology to species recovery in India. Biological Conservation 252:108846.

Karanth, K. U., J. D. Nichols, N. S. Kumar, W. A. Link, and J. E. Hines. 2004. Tigers and their prey: Predicting carnivore densities from prey abundance. Proceedings of the National Academy of Sciences of the United States of America 101:4854–4858.

Karanth, K. U., and James. D. Nichols. 2002. Monitoring tigers and their prey: A manual for wildlife researchers, managers and conservationists in tropical Asia. Centre for Wildlife Studies, Bangalore, India.

Karanth, U. K., J. D. Nichols, J. M. Goodrich, G. V. Reddy, V. B. Mathur, H. T. Wibisono, S. Sunarto, A. Pattanavibool, and M. T. Gumal. 2017. Role of Monitoring in Global Tiger

Conservation. Pages 1–13 *in* K. Karanth and J. Nichols, editors. Methods for Monitoring Tiger and Prey Populations. Springer, Singapore.

Kawanishi, K., G. R. Clements, M. Gumal, G. Goldthorpe, M. N. Yasak, and D. S. K. Sharma. 2013. Using BAD for good: How best available data facilitated a precautionary policy change to improve protection of the prey of the tiger Panthera tigris in Malaysia. ORYX 47:420–426.

Keeping, D., J. H. Burger, A. O. Keitsile, M. C. Gielen, E. Mudongo, M. Wallgren, C. Skarpe, and A. L. Foote. 2018. Can trackers count free-ranging wildlife as effectively and efficiently as conventional aerial survey and distance sampling? Implications for citizen science in the Kalahari, Botswana. Biological Conservation 223:156–169.

Keeping, D., and R. Pelletier. 2014. Animal density and track counts: Understanding the nature of observations based on animal movements. PLoS ONE 9:1–11.

Kerley, L. L., A. S. Mukhacheva, D. S. Matyukhina, E. Salmanova, G. P. Salkina, and D. G. Miquelle. 2015. A comparison of food habits and prey preference of Amur tiger (Panthera tigris altaica) at three sites in the Russian Far East. Integrative Zoology 10:354–364.

Kery, M., and J. A. Royle. 2015. Applied Hierarchical Modeling in Ecology: Analysis of distribution, abundance and species richness in R and BUGS: Volume 1: Prelude and Static Models. Academic Press. Elsevier Science.

Lomanov, I. K. 2000. Winter transect count of game animals for large territories: Results and prospects. Zoologicheskii Zhurnal.

Loonam, K. E., D. E. Ausband, P. M. Lukacs, M. S. Mitchell, and H. S. Robinson. 2021. Estimating Abundance of an Unmarked, Low-Density Species using Cameras. Journal of Wildlife Management 85:87–96.

Lubis, M. I., W. Pusparini, S. A. Prabowo, W. Marthy, Tarmizi, N. Andayani, and M. Linkie. 2020. Unraveling the complexity of human–tiger conflicts in the Leuser Ecosystem, Sumatra. Animal Conservation 23:741–749.

Massei, G., J. Coats, M. S. Lambert, S. Pietravalle, R. Gill, and D. Cowan. 2017. Camera traps and activity signs to estimate wild boar density and derive abundance indices. Pest Management Science 74:853–860.

Miquelle, D. G., J. M. Goodrich, E. N. Smirnov, P. A. Stephens, O. Y. Zaumyslova, G. Chapron, L. Kerley, A. A. Murzin, M. G. Hornocker, and H. B. Quigley. 2010. Amur tiger: a case study of living on the edge.

Miquelle, D. G., E. N. Smirnov, T. W. Merrill, A. E. Myslenkov, H. B. Quigley, M. G. Hornocker, and B. Schleyer. 1999. Hierarchical spatial analysis of Amur tiger relationships to habitat and prey.

Miquelle, D. G., E. N. Smirnov, H. B. Quigley, M. G. Hornocker, I. G. Nikolaev, and E. n. Matyushkin. 1996. Food Habits of Amur Tigers in Sikhote-Alin Zapovednik and the Russian Far East, and implications for conservation. Journal of Wildlife Research 1:138–147.

Miquelle, D., I. Nikolaev, J. Goodrich, B. Litvinov, E. Smirnov, and E. Suvorov. 2009. Searching for the coexistence recipe: a case study of conflicts between people and tigers in the Russian Far East. Pages 305–322 People and Wildlife. Cambridge University Press.

Miquelle, D., W. C. Society, and P. A. Stephens. 2005. CH A P T E R 1 0 Tigers and Wolves in the Russian Far East : Competitive Exclusion , Functional Redundancy , and Conservation Implications.

Moeller, A. K., and P. M. Lukacs. 2021. spaceNtime: an R package for estimating abundance of unmarked animals using camera-trap photographs. Mammalian Biology.

Moeller, A. K., P. M. Lukacs, and J. S. Horne. 2018. Three novel methods to estimate abundance of unmarked animals using remote cameras. Ecosphere 9.

Morelle, K., J. Bubnicki, M. Churski, J. Gryz, T. Podgórski, and D. P. J. Kuijper. 2020. Disease-Induced Mortality Outweighs Hunting in Causing Wild Boar Population Crash After African Swine Fever Outbreak. Frontiers in Veterinary Science 7.

Morin, D. J., J. Boulanger, R. Bischof, D. C. Lee, D. Ngoprasert, A. K. Fuller, B. Mclellan, R. Steinmetz, S. Sharma, D. Garshelis, A. Gopalaswamy, M. A. Nawaz, U. Karanth, N. Muhammad, A. Nawaz, and D. J. Morin. 2022. Comparison of methods for estimating density and population trends for low-density Asian bears. Global Ecology and Conservation 35:1–21.

Nakashima, Y., K. Fukasawa, and H. Samejima. 2018. Estimating animal density without individual recognition using information derivable exclusively from camera traps. Journal of Applied Ecology 55:735–744.

Nichols, J. D., and B. K. Williams. 2006. Monitoring for conservation. Trends in Ecology and Evolution 21:668–673.

Palencia, P., J. M. Rowcliffe, J. Vicente, and P. Acevedo. 2021. Assessing the camera trap methodologies used to estimate density of unmarked populations. Journal of Applied Ecology 58:1583–1592.

Petrunenko, Y. K., R. A. Montgomery, I. V. Seryodkin, O. Y. Zaumyslova, D. G. Miquelle, and D. W. Macdonald. 2016. Spatial variation in the density and vulnerability of preferred prey in the landscape shape patterns of Amur tiger habitat use. Oikos 125.

Pfeffer, S. E., R. Spitzer, A. M. Allen, T. R. Hofmeester, G. Ericsson, F. Widemo, N. J. Singh, and J. P. G. M. Cromsigt. 2018. Pictures or pellets? Comparing camera trapping and dung

counts as methods for estimating population densities of ungulates. Remote Sensing in Ecology and Conservation 4:173–183.

Piper, P. J., J. Ochoa, H. Lewis, V. Paz, and W. P. Ronquillo. 2008. The first evidence for the past presence of the tiger Panthera tigris (L.) on the island of Palawan, Philippines: Extinction in an island population. Palaeogeography, Palaeoclimatology, Palaeoecology 264:123–127.

Qi, J., J. Gu, Y. Ning, D. G. Miquelle, M. Holyoak, D. Wen, X. Liang, S. Liu, N. J. Roberts, E. Yang, J. Lang, F. Wang, C. Li, Z. Liang, P. Liu, Y. Ren, S. Zhou, M. Zhang, J. Ma, J. Chang, and G. Jiang. 2021. Integrated assessments call for establishing a sustainable meta-population of Amur tigers in northeast Asia. Biological Conservation 261.

Ripple, W. J., J. A. Estes, R. L. Beschta, C. C. Wilmers, E. G. Ritchie, M. Hebblewhite, J. Berger, B. Elmhagen, M. Letnic, M. P. Nelson, O. J. Schmitz, D. W. Smith, A. D. Wallach, and A. J. Wirsing. 2014. Status and ecological effects of the world's largest carnivores. American Association for the Advancement of Science.

Romani, T., C. Giannone, E. Mori, and S. Filacorda. 2018. Use of track counts and camera traps to estimate the abundance of roe deer in North-Eastern Italy: are they effective methods? Mammal Research 63:477–484.

Rowcliffe, J. M., J. Field, S. T. Turvey, and C. Carbone. 2008. Estimating animal density using camera traps without the need for individual recognition. Journal of Applied Ecology 45:1228–1236.

Rowcliffe, J. M., R. Kays, C. Carbone, and P. A. Jansen. 2013. Clarifying assumptions behind the estimation of animal density from camera trap rates. Journal of Wildlife Management 77:876.

Royle, J. A., A. H. Drive, and A. Roylefwsgov. 2004. N -Mixture Models for Estimating Population Size from Spatially Replicated Counts:108–115.

Royle, J. A., J. D. Nichols, K. U. Karanth, and A. M. Gopalaswamy. 2009. A hierarchical model for estimating density in camera-trap studies. Journal of Applied Ecology 46:118–127.

Schaub, M., and F. Abadi. 2011, September 1. Integrated population models: A novel analysis framework for deeper insights into population dynamics. Springer Verlag.

Schaub, M., O. Gimenez, A. Sierro, and R. Arlettaz. 2007. Use of integrated modeling to enhance estimates of population dynamics obtained from limited data. Conservation Biology 21:945–955.

Soofi, M., A. Ghoddousi, A. Kh. Hamidi, B. Ghasemi, L. Egli, A.-J. Voinopol-Sassu, B. H. Kiabi, N. Balkenhol, I. Khorozyan, and M. Waltert. 2017. Precision and reliability of indirect population assessments for the Caspian red deer Cervus elaphus maral . Wildlife Biology 2017:wlb.00230.

Stephens, P. A., O. Y. Zaumyslova, G. D. Hayward, and D. G. Miquelle. 2006a. Analysis of the long-term dynamics of ungulates in Sikhote-Alin Zapovednik, Russian Far East.

Stephens, P. A., O. Y. Zaumyslova, D. G. Miquelle, A. I. Myslenkov, and G. D. Hayward. 2006b. Estimating population density from indirect sign: Track counts and the Formozov-Malyshev-Pereleshin formula. Animal Conservation 9:339–348.

Tempa, T. 2017. The ecology of montane bengal tigers (Panthera tigris tigris) in the Himalayan Kingdom of Bhutan. University of Montana.

Tilson, R., K. Traylor-Holzer, and Q. M. Jiang. 1997. The decline and impending extinction of the South China tiger. ORYX 31:243–252.

Vinks, M. A., S. Creel, P. Schuette, M. S. Becker, E. Rosenblatt, C. Sanguinetti, K. Banda, B. Goodheart, K. Young-Overton, X. Stevens, C. Chifunte, N. Midlane, and C. Simukonda.

2021. Response of lion demography and dynamics to the loss of preferred larger prey. Ecological Applications 31.

Walston, J., J. G. Robinson, E. L. Bennett, U. Breitenmoser, G. A. B. da Fonseca, J. Goodrich, M. Gumal, L. Hunter, A. Johnson, K. Ullas Karanth, N. Leader-Williams, K. MacKinnon, D. Miquelle, A. Pattanavibool, C. Poole, A. Rabinowitz, J. L. D. Smith, E. J. Stokes, S. N. Stuart, C. Vongkhamheng, and H. Wibisono. 2010. Bringing the tiger back from the brink-the six percent solution. PLoS Biology.

Wikramanayake, E., E. Dinerstein, J. Seidensticker, S. Lumpkin, B. Pandav, M. Shrestha, H. Mishra, J. Ballou, A. J. T. Johnsingh, I. Chestin, S. Sunarto, P. Thinley, K. Thapa, G. Jiang, S. Elagupillay, H. Kafley, N. M. B. Pradhan, K. Jigme, S. Teak, P. Cutter, M. A. Aziz, and U. Than. 2011. A landscape-based conservation strategy to double the wild tiger population. Conservation Letters 4:219–227.

Wiles, G. C., O. Solomina, R. D'Arrigo, K. J. Anchukaitis, Y. V. Gensiarovsky, and N. Wiesenberg. 2015. Reconstructed summer temperatures over the last 400 years based on larch ring widths: Sakhalin Island, Russian Far East. Climate Dynamics 45:397–405.

Williams, B. K., J. D. Nichols, and M. J. Conroy. 2002. Analysis and Management of Wildlife Populations. Academic Press.

Wolf, C., and W. J. Ripple. 2016. Prey depletion as a threat to the world's large carnivores. Royal Society Open Science 3:1–13.

Wolf, C., and W. J. Ripple. 2017. Range contractions of the world's large carnivores. Royal Society Open Science 4.

Xiao, W., M. Hebblewhite, H. Robinson, L. Feng, B. Zhou, P. Mou, T. Wang, and J. Ge. 2018. Relationships between humans and ungulate prey shape Amur tiger occurrence in a core protected area along the Sino-Russian border. Ecology and Evolution 2018:1–17.

Zakharova, O. I., I. A. Titov, A. E. Gogin, T. A. Sevskikh, F. I. Korennoy, D. V. Kolbasov, L. Abrahamyan, and A. A. Blokhin. 2021. African Swine Fever in the Russian Far East (2019–2020): Spatio-Temporal Analysis and Implications for Wild Ungulates. Frontiers in Veterinary Science 8:1–13.

7 | TABLES & FIGURES

Table 1-1: Comparison of four methods to estimate densities of species the individuals of which cannot be uniquely identified. A brief explanation of the technique is given, along with the advantages, assumptions, and difficulties involved with each technique. Underlined references are considered foundational to the technique in its development and/or explanation. Other references are example applications of the technique since the model's development.

Method	Technique	Advantages	Assumptions & Difficulties	References
Formozov-Malyushev-Pereleshin Method (FMP)	• Winter track surveys conducted along transects, typically ~5-10km long. • Tracks <24h old are recorded by species and number of individuals	• Long history of use in Russia • Scientists gain additional information about species by following them through their habitat • Continuity of methods for long-term data sets in Russia • Method robust to animal movement tortuosity • Estimates apparently unaffected by double-counting of tracks	• Assumes animals move independent of transects • Depends on recurrent snowfall • Group size often difficult to determine • Impractical survey effort required for low densities • Assumes perfect species identification by tracks • Assumes tracks correctly ID'd as <24h old • Prone to convenience sampling • Assumes closed population • Prone to bias with inaccurate estimates of travel distance	• Lomanov 2000) • Stephens et al. 2006b • Keeping and Pelletier 2014) • Jousimo & Ovsaiken et al. 2016 • Petrunenko et al. 2016 • Romani et al. 2018 • Jiayin et al. 2018) • Ahlswede et al. 2019 • Doran-meyers et al. 2021
Random Encounter Model (REM)	• Uses camera traps • Estimates density based on two components: (1) animal encounter rate with cameras; and (2) the cameras' field of view (radius and angle of detection) • Equation very similar to and inspired by the FMP method (above)	• Minimal survey effort required to deploy cameras • Allows for animal movements non-independent of one another ((Rowcliffe et al. 2013) • Robust to assumption of random, independent animal movement	• Assumes camera viewsheds collectively represent the study area • Assumes random placement of cameras with respect to animal movement • Assumes closed population • Prone to bias with inaccurate estimates of travel distance • Requires estimates of camera viewshed, which are laborious to estimate (e.g. Hofmeester et al. 2017)	• Rowcliffe et al. 2008 • Chauvenet et al. 2017 • Massei et al. 2017 • Soofi et al. 2017 • Gray 2018 • Pfeffer et al. 2018 • Loonam et al. 2020a • Palencia et al. 2021 • Doran-meyers et al. 2021 • Morin et al. 2022
Space-To-Event Model (STE)	• Uses camera traps • Estimates density based on the amount of *space* sampled to the first observation for each sampling occasion; uses *spatial* trapping rate	• The camera's viewshed is the sample grid cell - eliminates detection probability within a larger cell • Robust to closed populations • Robust to the assumption of independent detection events	• Assumes camera viewsheds collectively represent the study area • Assumes animals are Poisson-distributed across camera viewsheds • Lower precision of estimates relative to other estimators • Assumes observations are independent between occasions *t* and *t+1* • Requires estimates of camera viewshed, which are laborious to estimate (e.g. Hofmeester et al. 2017) • With motion-trigger data, decisions about the sampling window length are arbitrary	• Moeller et al. 2018 • Loonam et al. 2020a • Ausband et al. 2022 • Morin et al. 2022
Time-To-Event Model (TTE)	• Uses camera traps • Elaboration of STE: the amount of space sampled before the 1st observation is isolated for each camera, calculated over many occasions (hence *time* to event at each camera).	• Able to account for heterogeneity in density • The camera's viewshed is the sample grid cell - eliminates detection probability • Robust to closed populations • Robust to the assumption of independent detection events	• Assumes random placement of cameras with respect to animal movement • Assumes animals are Poisson-distributed across camera viewsheds • Prone to bias with inaccurate estimates of travel distance • Assumes observations are independent between occasions *t* and *t+1* • Requires estimates of camera viewshed, which are laborious to estimate (e.g. Hofmeester et al. 2017)	• Moeller et al. 2018 • Loonam et al. 2020a • Ausband et al. 2022 • Morin et al. 2022 • Santini et al. 2022

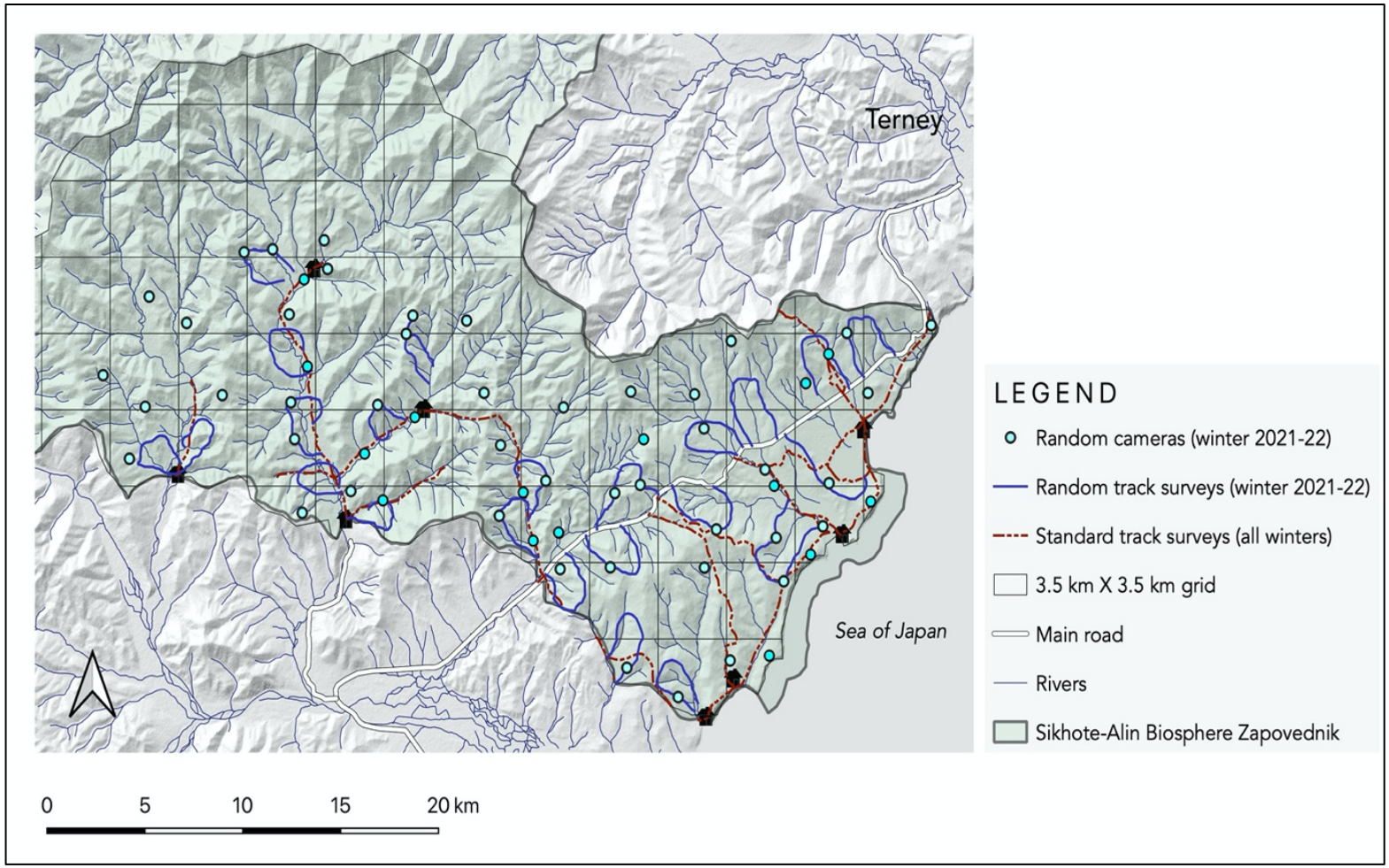

Figure 1-1. Locations of random cameras, and both the standard and random winter track surveys conducted in the southern portion of Sikhote-Alin Biosphere Zapovednik, Russian Far East. Only camera locations (N=62) and random track surveys (22 surveys totaling 168 km) from winter 2021-22 are shown (the three winters varied in their locations). The village of Terney is labeled to the northeast.

Table 1-2. Summary of survey efforts during winters 2019-20 and 2020-21 for both camera trap surveys and snow track surveys. See methods for more details about study design. During winter 2019-20, the number in parentheses after the brand of camera indicates the number of models of that brand that were used.

		Winter 2019-20	Winter 2020-21
Camera traps	Study dates	01-Feb-2020 – 01-Apr-2020	20-Nov-2020 – 10-Feb-2021
	Deployed N cams	50	57
	N cams used in analysis	45	50
	Total trap nights	2,743	4,050
	Brands of cameras	Bushnell (2) Reconyx (2) SPromise (2) Browning (2)	Panthera V7 Browning Recon Force
FMP random surveys	Dates of survey	27-Feb-2020 – 15-Mar-2020	--
	Total effort (km)	64	--
	N survey routes	8	--
FMP conventional surveys	Dates of survey	26-Feb-2020 – 02-Mar-2020	16-Feb-2021 – 27-Feb-2021
	Total effort (km)	103	117
	N survey routes	19	19

Table 1-3. Descriptions of criteria used to score camera trap and snow track survey estimators for their use to monitor prey of the Amur tiger. Criteria are grouped by the three broad categories of statistics, logistics, and costs of each estimator. More detailed descriptions and the scoring of each estimator are provided in Appendix 1C.

Category	Criterion	Score	Description
Statistics	Precision (CV)	1 - 4	Average CV of each estimator for each species and for the two seasons: 10-20%, 1; 20-30%, 2; 30-40%, 3; and 40%+, 4.
	Potential bias in parameters	1 – 4	Relative scores based on # of parameters in the estimator and their susceptibility to bias.
	Potential bias in study design	1 – 4	Relative score for camera traps and snow track surveys.
	Complexity of analysis	1 – 4	Relative scores based on both the number of analysis steps and their complexity.
Logistics	Difficulty in planning survey	1 – 4	Relative scores based on difficulty in implementation, considering staff, season, and weather-dependence.
	Difficulty of gear preparation	1 – 4	Relative scores preparing for sampling (deploying cameras or preparing for survey routes).
	Difficulty of site setup	1 – 4	Relative scores based on the stages involved in camera site setup (no penalty for track surveys).
	Difficulty preparing data for analysis	1 – 4	Relative scores based on complexity of preparing data for statistical analysis
Costs	Survey effort to achieve 20% CV	1 – 4	The number of cameras required to achieve this precision, based on simulations from our real data. For snow track surveys, we converted surveys into camera-equivalent effort (Appendix 1A).
	Start-up costs to achieve 20% CV	1 – 4	Cost to purchase the number of cameras to achieve 20% CV (determined above). No start-up penalties for track surveys.
	Stages of analysis	1 – 4	Rank based on the number of stages of analysis, from the processing of raw data (all camera trap images and notebooks with snow tracking data) to final density estimates.

Table 1-4. Values of parameters and other information used to estimate the densities of prey species during winter 2019-20 (February 01 – April 01, 2020; S1) and winter 2020-21 (November 20, 2020 – February 10, 2021; S2). Parameter symbology and definitions are explained in the Methods section.

		Wild boar		**Red deer**		**Roe deer**		**Sika deer**	
Method	**Parameter**	S1	S2	S1	S2	S1	S2	S1	S2
FMP Random	*Y/S* (tracks/km)	2.09	--	0.35	--	0.10	--	1.51	--
	v (km/day)	2.42 - 3.59		1.18 - 1.40		0.79 - 0.99		1.50 - 4.06	
	S (km)	63.8	--	63.8	--	63.8	--	63.8	--
FMP Trail	*Y/S* (tracks/km)	3.26	0.38	0.99	0.30	0.18	0.32	6.29	4.26
	v (km/day)	2.42 - 3.59		1.18 - 1.40		0.79 - 0.99		1.50 - 4.06	
	S (km)	103.2	116.9	103.2	116.9	103.2	116.9	103.2	116.9
REM	*Y/t* (detections/day)	0.067	0.002	0.011	0.021	0.004	0.011	0.019	0.023
	v (km/day)	2.42 - 3.59		1.18 - 1.40		0.79 - 0.99		1.50 - 4.06	
	r (km, median)	0.012	0.010	0.012	0.010	0.012	0.010	0.012	0.010
	theta (radians, mean)	0.820	0.960	0.820	0.960	0.820	0.960	0.820	0.960
STE	Occasion (min)	15		15		15		15	
	Sample window (sec)	7	60	60		60		7	
	Censor area (m^2)	1443	2502	1443	2502	1443	2502	1443	2502
	Non-NA STEs	14	1	3	8	1	5	9	15
TTE	Occasion (minutes)	1440		1440		1440		1440	
	Period (seconds)	189	260	499		624		208	
	N periods per occasion	24		24		24		24	
	Occasion length	14900	23250	14900	23250	14900	23250	14900	23250
	Non-NA TTEs	68	7	20	55	7	32	27	44

Table 1-5. Point density estimates and their coefficients of variation for ungulate prey species during winter 2019-20 (February 01 – April 01, 2020; S1) and winter 2020-21 (November 20, 2020 – February 10, 2021; S2). Random FMP surveys were not conducted during Winter 2020-21.

		Wild boar		**Red deer**		**Roe deer**		**Sika deer**	
Method	**Parameter**	S1	S2	S1	S2	S1	S2	S1	S2
FMP Random	*D* (ind/km^2)	1.02	--	0.42	--	0.17	--	0.80	--
	CV	32%	--	53%	--	63%	--	39%	--
FMP Trail	*D* (ind/km^2)	1.62	0.21	1.19	0.41	0.32	0.63	3.41	2.61
	CV	46%	45%	34%	44%	32%	39%	42%	44%
REM	*D* (ind/km^2)	3.27	0.11	0.92	1.91	0.49	1.35	0.89	1.13
	CV	31%	88%	38%	35%	43%	35%	53%	69%
STE	*D* (ind/km^2)	1.12	0.05	0.28	0.34	0.08	0.26	0.72	0.77
	CV	27%	124%	64%	41%	125%	48%	35%	26%
TTE	*D* (ind/km^2)	3.21	0.14	1.80	1.75	0.72	1.23	1.37	0.58
	CV	12%	40%	23%	14%	40%	18%	20%	15%

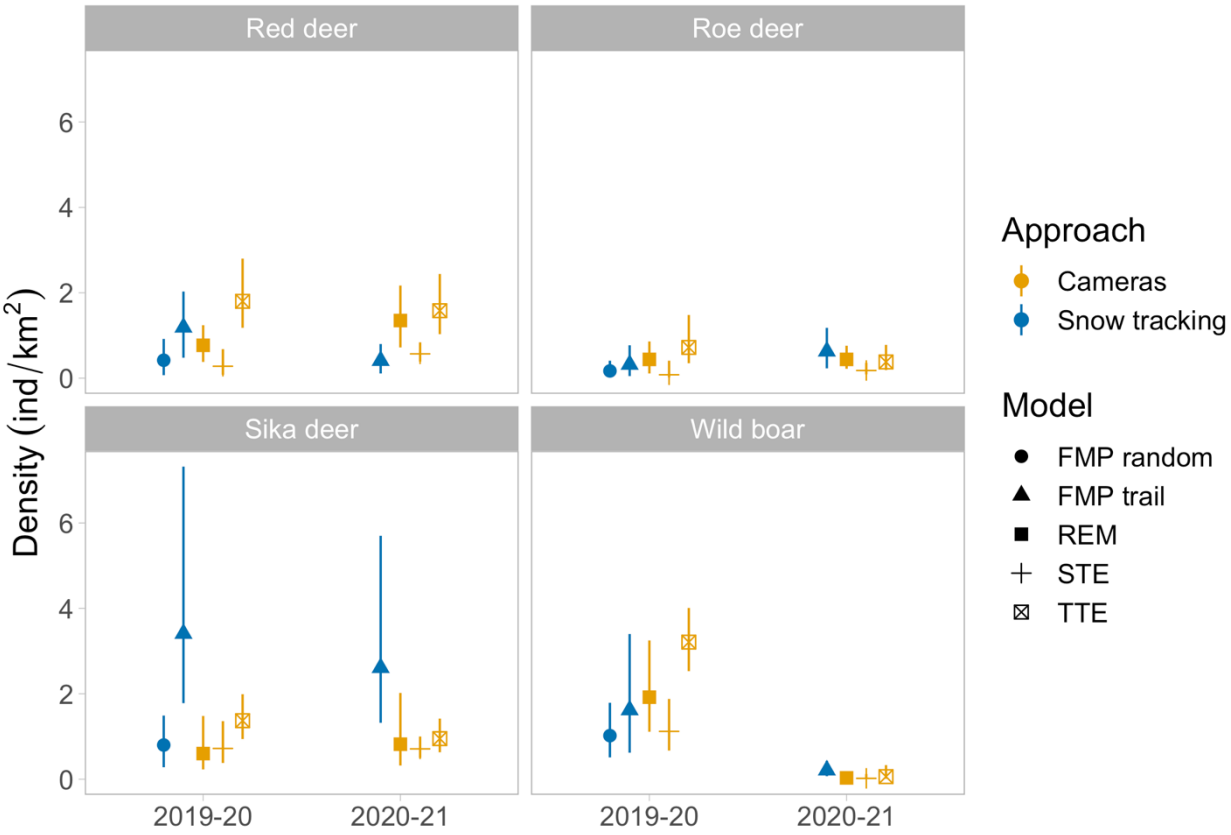

Figure 1-2. Estimates of population density with 95% confidence intervals for each prey species during winters 2019-20 (February 01 – April 01, 2020) and 2020-21 (November 20, 2020 – February 10, 2021). The two colors represent the two approaches to data collection: camera traps and snow track surveys. Each model is represented by a different shape at the point estimate. We were not able to conduct random snow tracking surveys during winter 2020-21.

Table 1-5. Scores for each density estimator based on the rubric described in Table 1-4. The information used and decisions made for each score are presented in Appendix 1C. The "data collection cost index" is not used to rank estimators, but is instead listed because of the context it provides readers.

	Criterion	Score	STE	TTE	REM	FMP
Statistics	Precision (CV)	1 - 4	4 (61%)	2 (23%)	4 (49%)	4 (47%)
	Potential bias in parameters	1 – 4	2	3	3	2
	Potential bias in study design	1 – 4	2	2	2	1
	Complexity of analysis	1 – 4	3	4	4	2
Logistics	Difficulty in planning survey	1 – 4	2	2	2	4
	Difficulty of gear preparation	1 – 4	3	3	3	1
	Difficulty of site setup	1 – 4	3	3	3	1
	Difficulty preparing data for analysis	1 – 4	3	4	4	2
Costs	Cameras to achieve 20% CV	1 – 4	3 (120)	2 (75)	4 (150)	1 (58)
	Start-up costs to achieve 20% CV	1 – 4	4 ($27,072)	3 ($16,920)	4 ($33,840)	1 ($0)
	Stages of analysis	1 – 4	3	4	4	2

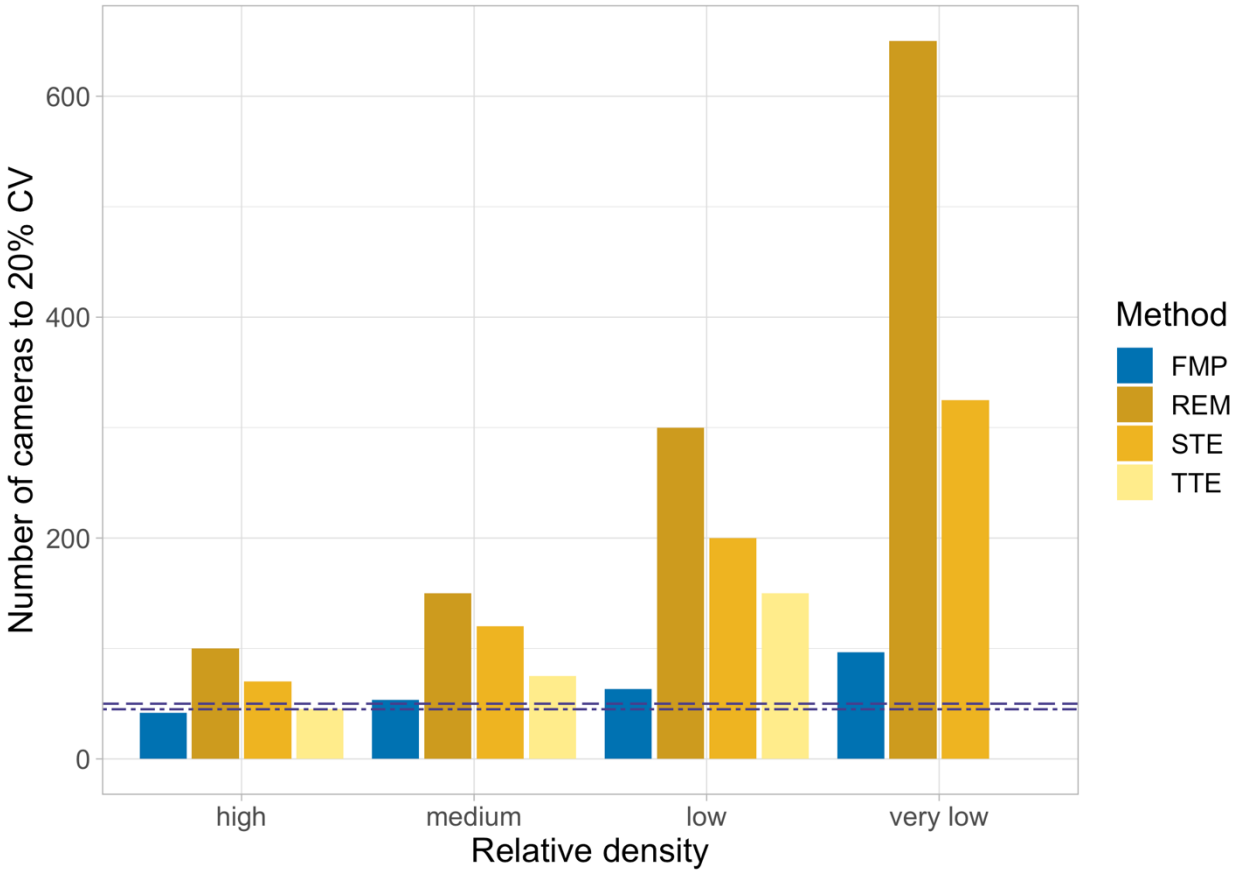

Figure 1-3. Simulated number of cameras or camera-equivalent survey effort for the three viewshed density estimators and FMP surveys, respectfully. Simulations used real data from the three winter seasons. Dot-dash lines represent the camera survey effort (N=45) from winter 2019-20, and the dashed line above represents the camera survey effort (N=50) from winter 2020-21.

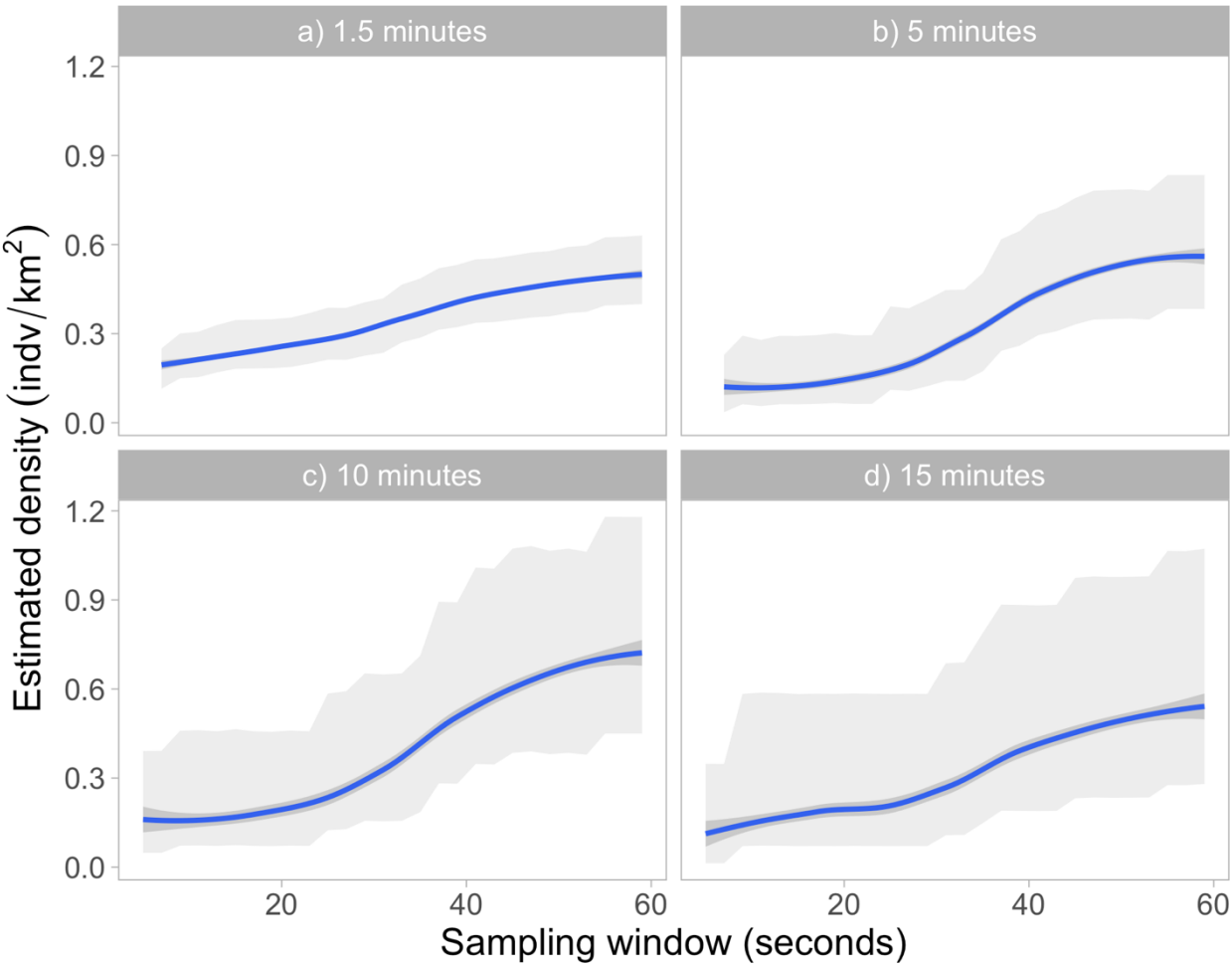

Figure 1-4. Sensitivity of Space-To-Event density estimates to increases in the sampling window length. This example figure is based on red deer detection data from the 2020-21 winter season, though the relationship is the same for all species and all seasons. Each panel (a-d) represent an increasing occasion length. As the sampling window increases, density estimates increase. As the occasion length increases, point estimates of density remain consistent, but precision decreases.

8 | APPENDICES

APPENDIX 1A: VIEWSHED AREA MEASUREMENTS

Winter 2019-20

During our first camera deployment season, we conducted extensive walk tests at each camera to determine the angles and distances to detection. We considered a distance as consistent if it detected at least one passage out of three. To measure angles, the first field technician would move to the outer edge of the detection zone. Once they identified the location of the maximum angle, the second field technician would take a bearing with a compass placed on top of the camera trap. This was repeated for the other side of the detection zone, and the detection angle thus estimated. This process was time consuming, often taking over 30 minutes, depending on the camera model and age, weather conditions, and terrain.

Winter 2020-21

During the winter 2020-21 deployment season, we tried an alternative approach to measuring viewshed area developed by Idaho Fish & Game biologists. First, 30cm X 40cm pieces of plywood were cut, and a dot drawn in the center of edge of the short side. Using a protractor and ruler, a pie shape was drawn according to the lens angle of a particular camera model. Next, that pie shape was divided into 6 equal sectors. Finally, small nails were tapped into the center of the edge of the widest part of each sector (away from the pie piece's origin). When in the field, one technician would kneel and place her head directly in front of the camera. Then, she would hold this "viewboard" to their forehead, such that their vision became divided into 6 equal sections. This technician would dictate to the other technician how far she could see in that sector. The other technician then measured the distance to the obstruction (such as a thick bush, rock, or tree).

If there were no obstructions, then the maximum detection distance was recorded. An example recorded data sheet is provided below (Figure A3).

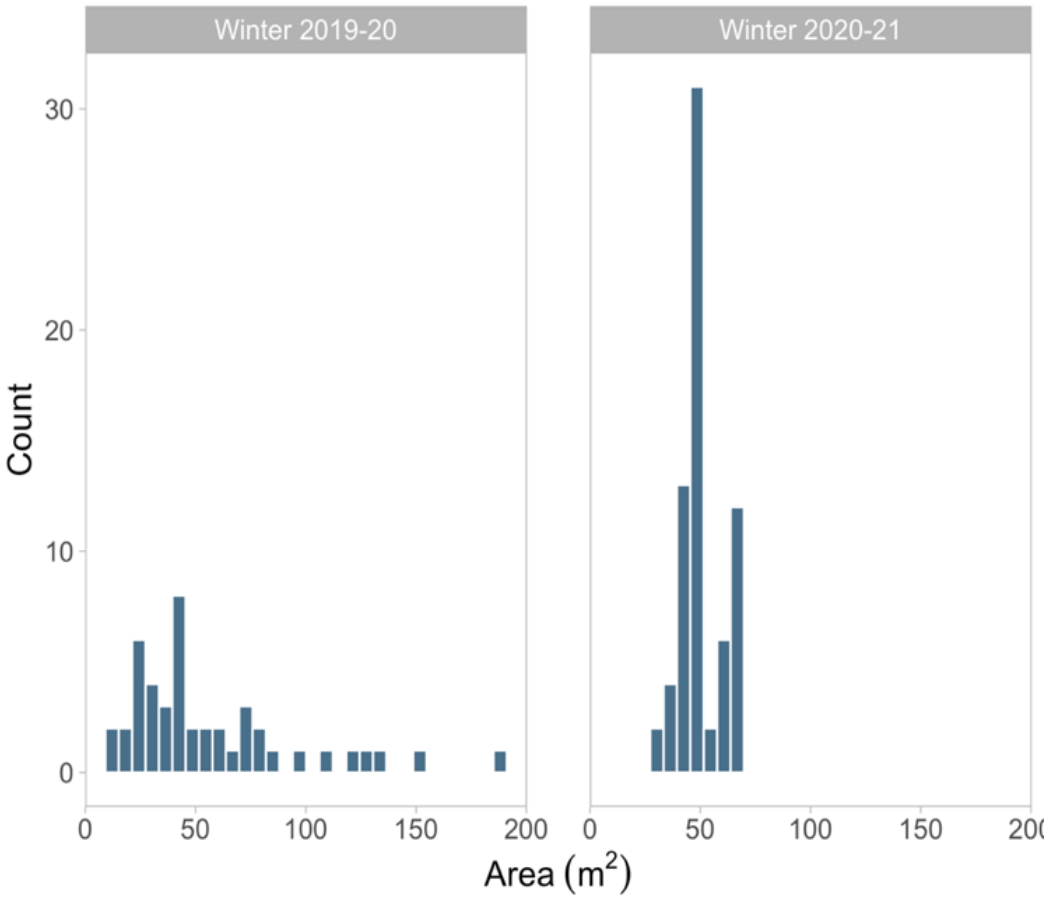

Figure A1. Histograms of individual camera viewshed areas measured during the winter 2019-20 and 2020-21 seasons.

APPENDIX 1B: ESTIMATING WILD BOAR DAILY TRAVEL DISTANCES WITH GPS RELOCATION DATA

Between the spring of 2019 and fall 2020, we captured 13 adult female wild boar in corral traps. We used a combination of Zoletil (6-9.2-mg/kg) and Medetomidine (0.07-mg/kg) to anaesthetize wild boar (Mikhail Goncharuk, pers comm), before fitting them with Lotek GPS Litetrack 420 Iridium collars set to a 15-minute fix interval schedule between November-1 and April-1. All captures and handling were conducted by WCS Russia and Zapovednik staff, and met IACUC animal care standards as approved by the University of Montana (AUP 061-19). Eight of these captured individuals contributed sufficient relocation data to estimate winter daily travel distances.

We estimated daily travel distance by summing the straight-line distances between points of an individual's relocation data during 24-hour periods (00:00:00 – 23:59:59). While this approach has been called into question (Noonan et al., 2019; Rowcliffe et al., 2016), previous analyses found no significant difference between this approach, the asymptotic approach used by Musiani et al. (1998) and the continuous time movement model estimates as described in Noonan et al. (2019) (Scott Waller, unpublished data). We used 1,000 iterations of nonparametric bootstrapping to estimate 95% confidence intervals of the median daily travel distance. We used values within the 95% confidence intervals as possible distances when estimating density with the REM and FMP in chapter 1.

Wild boar traveled a median daily distance of 3.1km in winter 2019-20 (N=487 days; Figure 4). This coincides with the early and later winter travel distances reported in Stephens et al. (2006). Most daily travel distances fell between 1-7 km. There were lots of acorns available

during this winter, as well as relatively little snow. As such, wild boar were able to forage freely, as described by the range of daily travel distances we estimated

This winter (2020-21), wild boar traveled a median daily distance of 2.3km (N=220), 0.9km less than the median of the previous winter. Most distances were between 0.5 – 4.5km. Importantly, much of this data was gathered while several of our wild boar were infected by, and eventually died from, African Swine Fever. This could partially explain the shorter distances traveled. What's more, this year there was little acorn mast available, as well as high snowfall and low temperatures. It makes sense then that our collared wild boar attempted to minimize energy expenditure, given challenges of disease infection, harsh environmental conditions, and little available resources.

REFERENCES

Musiani, M., H. Okarma, and W. Jedrzejewski. 1998. Speed and actual distances travelled by radiocollared wolves in Białowieża Primeval Forest (Poland). Acta Theriologica 43:409–416.

Noonan, M. J., C. H. Fleming, T. S. Akre, J. Drescher-Lehman, E. Gurarie, A. L. Harrison, R. Kays, and J. M. Calabrese. 2019. Scale-insensitive estimation of speed and distance traveled from animal tracking data. Movement Ecology 7.

Rowcliffe, J. M., P. A. Jansen, R. Kays, B. Kranstauber, and C. Carbone. 2016. Wildlife speed cameras: measuring animal travel speed and day range using camera traps. Remote Sensing in Ecology and Conservation 2:84–94.

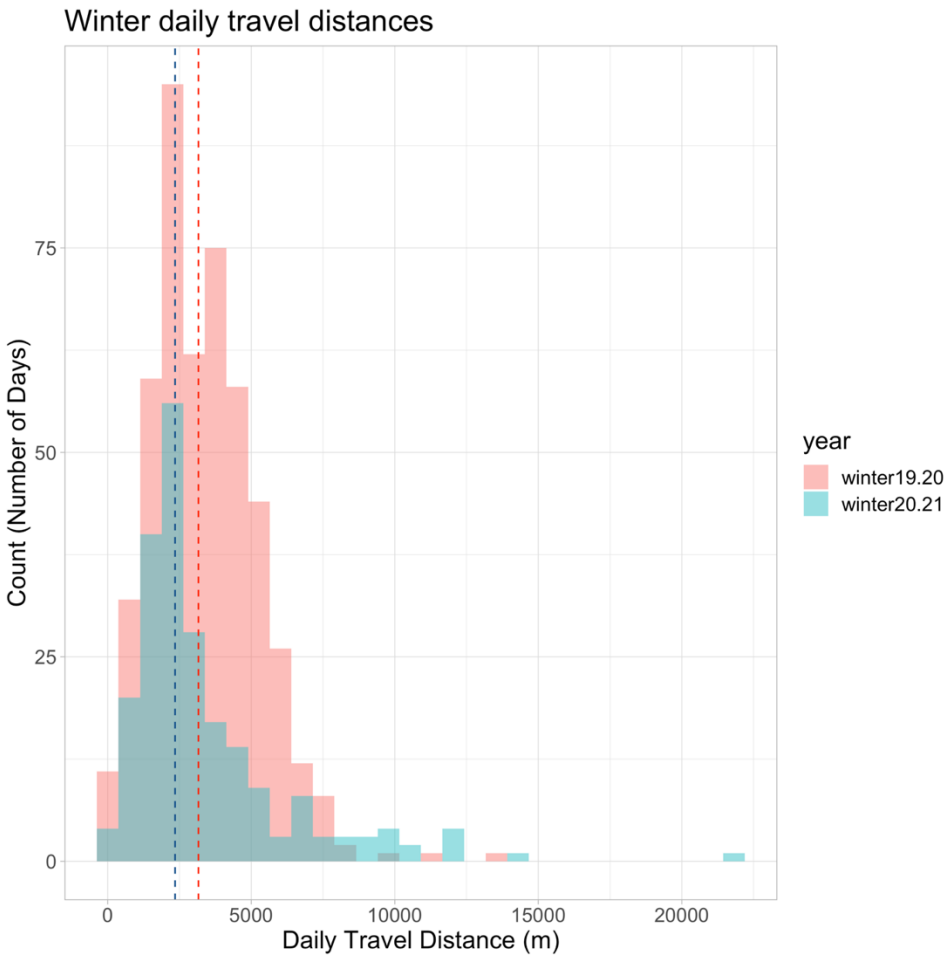

FIGURE 4. Histogram of daily travel distances for two winter seasons. Data are based on 487 and 220 estimated daily travel distances for winters 2019-20 and 2020-21, respectively. Dashed lines represent the median daily travel distances: for winter 2019-20, 3161 meters; for winter 2020-21, 2346 meters.

APPENDIX 1C: DETAILS OF RUBRIC SCORES FOR EACH ESTIMATOR

The following statistics, logistics, and cost categories and their respective criteria were adopted from Riley et al. (2017) and their comparison of methods to monitor Amur tiger populations.

STATISTICS

Precision

Rank each model based on their average coefficient of variation (CV) across species and years: 1 (10-20%), 2 (20-30%), 3 (30-40%), 4 (40%+).

- STE: 4 (61%)
- TTE: 2 (23%)
- REM: 4 (49%)
- FMP: 4 (47%)

Potential sources of bias in parameters

- STE: viewshed area, discontinuous sampling with motion-trigger: 2
- TTE: viewshed area, discontinuous sampling with motion-trigger, independent estimates of daily movement rate: 3
- REM: Viewshed radius and angle, discontinuous sampling with motion-trigger, independent estimates of daily movement rate: 3
- FMP: independent estimates of daily movement rate, only fresh tracks < 24h counted: 2

Potential sources of bias in study design

- STE: random camera placement, camera malfunctions: 2
- TTE: random camera placement, camera malfunctions: 2
- REM: random camera placement, camera malfunctions: 2
- FMP: placement of routes in study area: 1

Complexity of data analysis (steps)

NOTE: these steps are after the detection data has been processed and ready for analysis (track encounter data for FMP, species detections for viewshed density estimators), and camera deployment dataframe is prepared with accurate location, effort, and viewshed area data.

- STE: set parameter values (occasion and sampling window), build encounter history, run STE function: 3
- TTE: set parameter values (period length based on movement, sampling window, periods per occasion), build encounter history, run TTE: 4
- REM: parameterize animal movement rate, bootstrap density and variance: 3
- FMP: parameterize animal movement rate, bootstrap density and variance: 3

LOGISTICS

Difficulty planning for data collection

FMP: Because it can be so challenging to plan track surveys due to the weather, the FMP gets the worst score of 4. Cameras: 1 point each for planning deployment, and retrieval of cameras.

- STE: 2
- TTE: 2
- REM: 2

Difficulty of gear preparation

- STE: put memory cards and batteries in cameras, check settings are correct: 2
- TTE: put memory cards and batteries in cameras, check settings are correct: 2
- REM: put memory cards and batteries in cameras, check settings are correct: 2
- FMP: no gear preparation beyond any requirements for being in the field : 1

Difficulty of site set-up

- STE: choosing the location of the camera and placing correctly, measuring viewshed area, turning on camera: 3
- TTE: choosing the location of the camera and placing correctly, measuring viewshed area, turning on camera: 3
- REM: choosing the location of the camera and placing correctly, measuring viewshed area, turning on camera: 3
- FMP: no sites involved: 1

Expertise required

- STE: only basic knowledge of how to use a GPS needed: 1
- TTE: only basic knowledge of how to use a GPS needed:: 1
- REM: only basic knowledge of how to use a GPS needed: 1
- FMP: expert assessment of track species and age, but this can be trained relatively easy especially for large ungulate prey species: 3

Difficulty preparing collected data for analysis (steps)

- STE: delete empty images, identify species correctly, calculate camera area: 3
- TTE: delete empty images, identify species correctly, calculate camera area, estimating movement: 4
- REM: delete empty images, identify species correctly, calculate camera area, estimating movement: 4
- FMP: record surveyor's written data, estimate animal movement: 2

COSTS

Simulated effort to achieve 20% CV

To fully understand the effort required to deploy the number of cameras our simulations indicated to achieve 20% CV for various densities, we estimated the fieldwork travel that would be required to deploy the indicated number of cameras, based on survey efforts during winter 2021-22. That year, field crew walked a total of 360 km and drove 156 km to deploy 62 cameras, which amounts to 8.4 km of total field travel for each camera trap deployed. To make our simulations of effort comparable between camera traps and snow track surveys, we divided the simulated kilometers of snow track surveys by 8.4. This represented the snow track survey efforts in units of camera-equivalents. We also recorded the km driven by snowmobiles or 4-wheelers during this survey, which gave us an average survey length of 7.7 km for each track survey, or roughly 0.91 cameras deployed during each survey. This information is useful, but because we are already scoring estimators based on the number of cameras or camera-equivalent effort, we did not include this in the rubric.

For the rubric scores, we used simulated effort values based on the medium density species. The results of all simulations are presented in Figure 1-4 (pg. 46). Note that this approach favors camera trapping, because we do not account for the equivalent effort required to retrieve those cameras.

Number of cameras (camera equivalent effort for FMP) to reach 20% CV for density of 0.7 km^{-2}:

- STE: 120 – 3
- TTE: 75 – 2
- REM: 150 – 4
- FMP: 54 – 1

Start-up costs:

- STE: 120 cameras @ $200 each, 120 memory cards @ $8 each, 960 lithium AA batteries (8 per camera) @ $2.2 per battery: **total = $27,072**: 4
- TTE: 75 cameras @ $200 each, 75 memory cards @ $8 each, 600 lithium AA batteries (8 per camera) @ $2.2 per battery: **total = $16,920**: 3
- REM: 150 cameras @ $200 each, 150 memories @ $8 each, 1,200 lithiium AA batteries (8 per camera) @ $2.2 per battery: **total = $33,840**: 4
- FMP: nothing beyond typical field work gear. **Total = $0**: 1

Stages of analysis

- STE: saving and recording data from camera memory cards, cleaning empty photos, tagging photos and creating detection file, statistical analysis: 4
- TTE: saving and recording data from camera memory cards, cleaning empty photos, tagging photos and creating detection file, statistical analysis: 4
- REM: saving and recording data from camera memory cards, cleaning empty photos, tagging photos and creating detection file, statistical analysis: 4
- FMP: record track data written in surveyor booklets, statistical analysis: 2

Table C1: Average scores for each estimator in each category.

	STE	TTE	REM	FMP	Mean
Statistics	2.8	2.8	3.3	2.3	2.8
Logistics	2.8	3.0	3.0	2.0	2.7
Costs	3.3	3.0	4.0	1.3	2.9
Total	**2.9**	**2.9**	**3.4**	**1.9**	**2.8**

CHAPTER 2: COMPARING ROAD, OFF-ROAD, AND RANDOMLY PLACED CAMERA TRAPS: LINEAR FEATURES BIAS DETECTIONS OF LARGE UNGULATES

1 | INTRODUCTION

Random sampling is an essential tool in scientific research. The degree to which a sample of observations represents the study population in an unbiased way determines the quality of our statistical inferences (Fisher 1925, Cochran 1977, Garton et al. 2012). Random sampling ensures that we achieve a sample of the population that does not bias estimates of the sample mean and variance by sample selection (Cochran 1977, Jolly 1979, Williams et al. 2002). In the field of population ecology, researchers make inferences about a study population of a species based on parameters estimated from, ideally, a random sample of that population (Garton et al. 2012, Mills 2013). Estimates of the true abundance of a population are especially valuable as it allows managers to monitor trends over time and thus assess the consequences of management and conservation actions (Williams et al. 2002). Population size and trends are also key metrics by which the IUCN categorizes a species' threat status (IUCN 2012). Because of the value of abundance estimates, much effort has been spent on its accurate, precise, and efficient estimation (Williams et al. 2002). Random sampling is often a key component of proposed methods to estimate abundance because it ensures the sample is representative of study population (Jolly 1979, Williams et al. 2002).

For over 100 years, ecologists have used the unique markings of individuals to estimate population size. Danish biologist C.G.J. Petersen was one of the first in the field of population ecology to apply mark-recapture techniques in 1889, though not for abundance purposes. His approach was later developed by F.C. Lincoln as the Lincoln-Petersen index to estimate abundance of waterfowl populations in the United States based on capture-recapture of randomly

marked individuals (Lincoln 1930, le Cren 1965, Mills 2013). Recently, spatially explicit capture-recapture (SECR) models were developed to make use of repeated detections of individuals within their home ranges to estimate the distribution of individuals across a study area. This provides a robust and well-tested means of estimating both abundance in a capture-recapture framework and, critically, the area of sampling (Efford et al. 2009, Royle et al. 2009).

Estimating abundance of unmarked populations has proven more difficult. Over the years, methods proposed have ranged from sightability models (Steinhorst and Samuel 1989), drive counts (Borkowski et al. 2011, Keuling et al. 2018), and distance sampling (Buckland et al. 2015). These models all assume that animals are observed in places representative of the study area, and randomly distributing routes, drives, or transects is a common technique. A major disadvantage of these ground-based models is that animals must be visually observed, and in the case of drive counts, in an area with clearly defined borders. But many wildlife populations of interest are hunted and therefore wary of humans, exist at densities too low to obtain sufficient observations, or live in thick vegetation and rugged terrain that make observing individuals infeasible.

One important example of the need for and challenges with estimating abundance of unmarked species is monitoring prey species for the conservation of wild tigers (*Panthera tigris*). Tiger density is ultimately dependent upon prey density across the tiger's range, and estimates of true population size – beyond relative abundance – has allowed researchers to describe this dependency (Karanth et al. 2004, Miquelle et al. 2010) and identify areas where insufficient prey limit tiger recovery (Harihar et al. 2020, Qi et al. 2021). Most prey species cannot be uniquely identified, and distance sampling is limited to only certain places in tiger range such as India (Karanth and Nichols 2002). Most countries still have not developed rigorous tiger prey monitoring programs, a major goal identified during the 2010 Global Tiger Summit (Global Tiger

Initiative 2010). Many tiger managers are using cameras and SECR models to monitor tiger densities (Tempa et al. 2019, Harihar et al. 2020, Jhala et al. 2020, Matiukhina 2020). These cameras coincidentally capture images of prey species, and some researchers have already estimated relative abundances of prey based on this "by-catch" data (Tempa 2017, Xiao et al. 2018, Kafley et al. 2019). However, the *N*-mixture models (Royle 2004) used in these analyses make strict assumptions that ultimately mean they cannot be interpreted as estimates of true abundance (Kery and Royle 2015, Gilbert et al. 2020).

The recent unmarked estimators developed to estimate true abundance with cameras also make the strict assumption that the area sampled in front of cameras (i.e., the "viewshed") is representative of the study area (Gilbert et al. 2020). Randomly placing cameras is a basic approach to meet this assumption when applying these methods, and has been used successfully to estimate densities of diverse wildlife populations (Rowcliffe et al. 2008, Howe et al. 2017, Moeller et al. 2018, Morelle et al. 2020, Palencia et al. 2021). While random sampling is expensive and takes more effort than placing cameras on roads and trails (see Chapter 1 of this thesis), cameras placed on linear features likely violate this important assumption of representative sampling. Past studies have investigated the differences between randomly placed cameras and cameras placed on linear features (e.g. Harmsen et al. 2010, Cusack et al. 2015, Kolowski and Forrester 2017, Tanwar et al. 2021). Yet most of these examples have focused on community-scale camera trap analyses such as species accumulation curves and measurements of species richness. Those that compared detection rates between camera deployment strategies found that differences between them vary widely depending on the study area and species (e.g., Tanwar et al. 2021). There remains a need to directly assess the differences in detections between

cameras placed on targeted features, and those deployed to represent the study area, such as through random sampling.

The studies mentioned above also did not account for the potential confounding effects of lower abundance and avoidance of human use of those roads and trails. Many studies have demonstrated that wildlife across diverse taxa avoid roads, especially with high levels of human use (Vistnes and Nellemann 2001, Jaeger et al. 2005, Northrup et al. 2012, Thurfjell et al. 2015). The avoidance of humans on roads and trails where camera traps are placed may therefore confound abundance when interpreting detection rates. Though evidence is accumulating that detections of many species are influenced by linear features, the degree to which sampling along such features leads to biased density estimates of unmarked populations remains unclear.

In this study, we assessed the importance of representative sampling and the influence of linear features in camera trap studies of population abundance by comparing relative abundance indies (RAIs) from three different deployment strategies:

1. Pairs of cameras placed in one location for tiger density monitoring ("road cameras");
2. Single cameras placed 150 m from tiger monitoring cameras, in a random direction and without targeting landscape features to attract animals ("off-road cameras");
3. Single cameras placed using a systematic random sampling design ("random cameras").

We compared RAIs of four ungulate species that are the main prey of the Amur tiger (Miquelle et al. 2010): wild boar (*Sus scrofa* ssp. *ussuricus*), red deer (*Cervus canadensis* ssp. *xanthopygus*), roe deer (*Capreolus pygargus*), and sika deer (*Cervus nippon*). We recognize that RAIs sometimes fail to detect trends in abundance or compare relative abundances among species (Harmsen et al. 2010, O'Brien 2011, Sollmann et al. 2013). However, our purpose was to compare camera deployment strategies that differed most meaningfully in the number of

detections of animals. Most of the variation in unmarked estimators comes from detection rates (Palencia et al. 2021). Thus, our comparison of RAIs should be relevant to researchers estimating densities of unmarked populations with cameras. Lastly, to understand how human use of roads and trails might affect detection rates of ungulates, we investigated how levels of low or high human traffic on roads where we placed cameras for monitoring tigers influenced estimates of ungulate RAIs.

2 | MATERIALS AND METHODS

2.1 Study Area

We deployed cameras in three study sites in central Sikhote-Alin, Russian Far East (Figure 1-1). The dominant geographical feature in this region is the low-elevation Sikhote-Alin Mountains that run parallel with the coast of the Sea of Japan. East of the divide, coastal forests of Mongolian oak (*Quercus mongolica*) transition to mixed hardwood forests with larch (*Larix* spp.) and Korean pine (*Pinus koreinsis*). These forests predominate our southern and eastern study sites in the Sikhote-Alin Biosphere Zapovednik (SABZ) (Figure 2-1). Across the Sikhote-Alin Mountains, forests are more coniferous with Korean pine, spruce (*Picea* spp.), and fir (*Abies* spp.), though diverse hardwood species such as Japanese poplar (*Populus maximowiczii*) and cork bark elm (*Ulmus propinqua*) grow in the riparian valleys. These forests characterize both the Sidatun Hunting Lease (Sidatun) and Udege Legend National Park (ULNP) study sites where we deployed additional road and off-road cameras (Figure 2-1).

The large mammal community in this system contains seven species of ungulates and multiple predators. Wild boar, red deer, roe deer, and sika deer are the predominant ungulate prey species, though less-common goral *(Naemorhedus caudatus*) inhabit the coastal cliffs and musk deer (*Moschus moschiferus*) occur in the spruce-fir forests of northern slopes. Sika deer are only

common along the coast of the Zapovednik, though their range is expanding (Stephens et al. 2006). Across the Sikhote-Alin Mountains, both red deer and roe deer are more abundant. Moose (*Alces alces*) are rare, especially in SABZ. Wild boar abundance fluctuates depending on the availability key mast crops, namely acorns from Mongolian oak along the coast and pine nuts from Korean pine further inland (Heptner et al. 1988). Amur tigers are the dominant predator in the community, often excluding wolves (*Canis lupus*) from their territory (Miquelle et al. 2005), and sometimes preying on both brown bears (*Ursus arctos*) and Himalayan black bears (*Ursus thibetanus*) as well as ungulate species (Miquelle et al. 1996, Kerley et al. 2015).

2.2 Road camera deployment

We deployed pairs of remote cameras at each site for tiger population monitoring in SABZ, ULNP, and Sidatun (Figure 2-1). Using a 7 × 7 km grid across the entire study area, one pair of cameras was placed in each cell. Camera sites were selected to maximize detections of tigers along roads, trails, and ridges, and facing tiger marking trees if present. Cameras were placed roughly 4 m away from and on either side of the road (no more than 100 m apart) to photograph both sides of passing tigers and were no more than 100 m apart from each other. Cameras were set to capture bursts of 3 photos with minimum trigger delay.

2.3 Off-road camera deployment

To test a deployment strategy that balances the need for random camera placement and logistical constraints, we deployed single cameras roughly 150 m away from each pair of tiger monitoring cameras and at least 100 m from the road itself. Typically, field staff alternated whether they went up steep slopes on one side of the road, or further into the river valley on the other side. For

camera site selection, field staff chose areas with minimal brush and other obstructions while avoiding features like game trails.

2.4 Random camera deployment

In the 527 km^2 southern SABZ study site (Figure 2-1), we deployed cameras using a systematic random sampling design to serve as a reference for unbiased estimates of RAIs. First, a rectangular 3.5 × 3.5 km grid was drawn over our study area. This cell size approximates the area of a female red deer's home range (Dou et al. 2019). We randomly generated one camera location in each cell, then excluded cameras that were not within the study area. Because of the remoteness of some cells, a few cameras' locations were adjusted to be more easily accessed, while maintaining the random location's forest type, elevation, and aspect. Because of resource constraints, if a pair of tiger monitoring cameras occurred within a cell, we only placed an off-road camera in that cell.

Both off-road and random cameras were placed 1 – 1.5 m above the ground and facing north to minimize glare from the sun. Whenever the camera site was on a slope, the camera was positioned such that its horizontal field of view was in-line with the slope to minimize reductions in detection area (Moeller et al. 2018; Appendix 1A, Figure A3). Cameras were set to take bursts of three photos at each capture with no delay. We considered detections of individuals of the same species 30 minutes apart to be independent events.

2.5 Estimating Relative Abundance Indices (RAIs)

The value of using an RAI instead of only the number of detections at a camera is that RAIs adjust those detections by the number of days that camera was operational (O'Brien 2011). In

most applications, RAIs are calculated for individual cameras, then averaged across sites for a mean RAI:

$$RAI = \frac{\sum_{i=1}^{N}\left(\frac{y_i}{t_i} \times 100\right)}{N} \qquad \text{Equation 1}$$

Where y_i is the number of independent detections at camera *i,* t_i is the number of days camera *i* was operational, and N is the total number of cameras.

While the estimation of RAIs using Equation 1 is widespread (Johnson et al. 2006, O'Brien 2011, Gilbert et al. 2020, Tanwar et al. 2021), our RAIs were always negative-exponentially distributed across study sites and seasons. Medians are a better summary statistic for skewed distributions, as means can be heavily biased by outliers. We therefore fit exponential distributions to RAIs of a study site using maximum likelihood estimation to estimate the rate parameter of the distribution, lambda (λ). The median *M* of an exponential distribution can be estimated by evaluating the integral of the probability density function from zero to *M*, then taking the logarithm of the reciprocal such that:

$$M = \lambda \ln(2) \qquad \text{Equation 2}$$

Finally, we used 1,001 iterations of nonparametric parametric bootstrapping (Efron and Tibshirani 1993) to estimate the median RAI and associated standard error.

For random and off-road cameras, we used bootstrapping to estimate the median RAI and its standard error. For road cameras, we had to additionally account for the difference in detections between the pair of cameras at one location, since they were up to 100 meters apart and thus sometimes had variable numbers of detections. To estimate an RAI for one location with a pair of cameras, we simply took the average of the individual camera RAIs. The paired cameras often had similar numbers of detections, and if there was a large difference, then we assumed the average adequately represented the variation between them.

2.6 RAI comparisons

To assess the importance of representative sampling and the influence of linear features on detection rates of ungulates, we first calculated RAIs from random cameras as a reference, unbiased estimate. We then calculated RAIs for road and off-road cameras, and compared these estimates to the random cameras. Note that all the cameras in this first analysis were within the southern SABZ study area (Figure 2-1). We then used linear mixed-effects models (Raudenbush & Bryk 2002) to test whether off-road and road RAIs were significantly different from random RAIs, with a random intercept for year. To better understand the differences between road and off-road RAIs alone, we expanded our study area and used linear mixed-effects models to compare differences in RAIs in the eastern SABZ, ULNP, and Sidatun study areas. In this second analysis, we used a random intercept for study area and, since we had multiple years of cameras in eastern SABZ, study year.

2.7 Effects of human road traffic on relative abundance of prey

To understand how detections of prey species on roads and trails were affected by the amount of human traffic on those linear features, we first estimated RAIs using the detections of humans, vehicles, and logging machinery at camera sites, using equation 1 above. These RAIs were summed together as a total human traffic index for each camera site. If the human traffic index was less than 75 detections per 100 days, that site was categorized as “low traffic”; if the index was equal to or greater than 75 detections per 100 days, the camera was categorized as “high traffic.” Because of the low sample of camera sites with high human traffic, we analyzed the relationship between prey RAIs and human traffic indices by including data from the years 2018-19, 2019-20, and 2020-21, and across our three study regions. We additionally included indices

from camera sites in the Terney hunting lease, to the east of SABZ (Figure 2-1), for a total of 295 camera sites. We then used linear regression to test for a significant effect of human traffic on individual prey species RAIs, as well as a combined prey RAI.

2.8 Data processing and analysis

RAIs were calculated using the R programming language in R (R Core Team 2022). After raw camera trap images were processed by field staff, detection data was produced in R using the *camtrapR* package (Neidballa et al. 2016). We used the *fitdistrplus* package in R to fit exponential distributions to the RAIs from different study sites (Delignette-Muller and Dutang 2015).

3 | RESULTS

We deployed cameras at 262 different locations over three years across the three study sites, and estimated 53 separate RAIs across prey species, deployment strategies, and study sites (Table 2-1). Seasons were each 60 days with the following dates: winter 2019-20, February 10 – April 10, 2020; winter 2020-21, October 10 – December 10, 2021. Season 3, (TBD). We picked these dates to minimize changes in animal movement and thus detection rates, as abundance and movement are confounded when using RAIs (Broadley et al. 2019).

In our comparison of RAIs estimated from cameras placed by representative sampling ("random"), targeting linear features for tiger monitoring ("road"), and restricting cameras to 150 m from roads ("off-road"), our linear mixed-effects models found both road and off-road RAIs to be consistently higher than random RAIs (Table 2-2). For instance, our regression analysis of roe deer found both road RAIs (β_{road} = 1.66, SE = 0.07, $p < 0.001$) and off-road RAIs ($\beta_{off-road}$ = 1.79, SE = 0.05, $p < 0.001$) were significantly greater than random RAIs (β_{random} = 0.87, SE = 1.13), with road and off-road RAIs being roughly double the reference random RAIs. The

exception to this was red deer, with off-road RAIs (β_{road} = 1.30, SE = 0.09, p = 0.99) being nearly identical to the random RAIs intercept ($\beta_{off-road}$ = 5.77, SE = 6.05).

In our further comparison of road and off-road RAIs including eastern SABZ, Sidatun, and ULNP (Figure 2-1), our regression models found road RAIs were significantly greater than off-road RAIs (Table 2-3) for all species. The strongest difference was for sika deer, with road RAIs (β_{road} = 3.85, SE = 0.09, $p < 0.001$) being close to three times greater than off-road RAIs ($\beta_{off-road}$ = 1.42, SE = 0.14). The weakest difference was for roe deer, as road RAIs (β_{road} = 0.30, SE = 0.02, $p < 0.001$) were only slightly greater than off-road RAIs ($\beta_{off-road}$ = 1.46, SE = 0.55), though this difference was still significant.

In our assessment of the effects of human traffic on prey relative abundance, our analysis was limited because only 27 cameras (9%) of the 295 cameras classified as high traffic. Still, we found that high traffic generally had a negative effect on prey RAIs, both for individual species and for the combined prey index (Figure 2-4, Table 2-4). For instance, red deer RAIs decreased by over 50% on roads with high traffic ($\beta_{high\ traffic}$ = -5.66, SE = 2.36, p = 0.02) compared to roads with low traffic ($\beta_{low\ traffic}$ = 10.19, SE = 0.72). In contrast, roe deer showed a slight increase in RAI estimates on roads with high traffic ($\beta_{high\ traffic}$ = 1.37, SE = 0.83, p = 0.10) compared to low traffic ($\beta_{low\ traffic}$ = 2.74, SE = 0.25), though this difference was insignificant.

4 | DISCUSSION

Many research techniques in biology depend on random sampling to obtain unbiased observations of the population of interest (Cochran 1977, Jolly 1979), and the recent models proposed to estimate densities of unmarked populations using camera traps are no exception (Gilbert et al. 2020). For wildlife managers who wish to implement these viewshed density estimators, this

translates to significant amounts of resources spent deploying and retrieving cameras across challenging terrain (see Chapter 1). Because camera traps are typically placed on roads and trails to maximize the detections of certain species (O'Brien 2011), many researchers may be tempted to gloss over the assumption of representative sampling and place cameras on roads and trails anyways. Or, as in the case with tiger managers, they may wish to use "by-catch" images of prey species from tiger monitoring cameras as data to estimate prey abundance. We found clear evidence that placing cameras on roads and trails leads to greater detection rates of large ungulates (Figure 2-2, Table 2-2). This aligns with previous work in other systems that demonstrated higher detections for most species on roads versus trails (Cusack et al. 2015b), though the opposite is sometimes true (Tanwar et al. 2021). Even in our attempt to approximate randomness by moving 150-meters away from tiger monitoring cameras, these cameras collectively still had higher detection rates than random cameras for most species (Figure 2-2).

The most probable cause of greater estimated RAIs at off-road cameras than random cameras was species' selection for lower-elevation habitats. Our random cameras sampled across all elevations in our study area, while off-road cameras were restricted to relatively lower elevations in forested river valleys. Hebblewhite et al. (2014) found that all four prey species selected habitats with the same characteristics as these roads and trails where road cameras were placed. This makes sense as in winter 2019-20 in SABZ, low elevation areas had the quickest melting of snow and green-up, while during periods of snow in winters 2020-21 and 2021-22, prey species likely restricted their movements to lower elevations where there was less snow and wind and warmer temperatures. Some of our highest elevation random cameras had no detections of prey species. While many of our off-road cameras were placed on steep slopes, they still were not far from valley bottoms and therefore likely had higher capture probabilities than high-

elevation random cameras. One possible solution would be to stratify the study area by elevation class and extend the 150 m distance for certain off-road cameras such that all elevation classes are adequately represented. However, this would also require more effort in planning and on the part of field staff, and reaching those high-elevation locations are the most time-consuming, tiresome, and dangerous.

Differences in detection rates between cameras are the main source of variance in unmarked density estimators (Palencia et al. 2021). This may be affected by differences in either actual local abundance or in animal movement patterns (Neilson et al. 2018, Broadley et al. 2019). The greater detections at road cameras compared to off-road and random cameras are likely a result of selection for roads, and greater movement speeds on roads. Animals from diverse taxonomic groups are known to behave differently on roads compared to off-road (e.g. Roever et al. 2010). At our study sites, prey species likely used roads to cover the study area more efficiently and to avoid areas of deep snow. We expect wild boar especially used roads to travel large distances while investigating pine nut and acorn mast crop quality, and this was reflected in the higher wild boar RAIs on roads compared to off-road in ULNP (Figure 2-3). In contrast, we do not think the differences between off-road and random cameras were due to micro-site characteristics of the cameras, but instead had to do with spatial and temporal variation in abundance (e.g. avoidance of high-elevation areas). This emphasizes the importance of tools like random sampling in unmarked estimators to ensure the study area is sufficiently represented.

While different movement behavior on roads may have influenced the differences in RAIs between random cameras and road cameras, our analysis of traffic effects on RAI estimates indicate that human activity also decreases detection rates. Both wild boar and red deer RAIs decreased on roads that had high levels of human use (Figure 2-4, Table 2-4), though our sample

size of roads with high levels of use was small. When interpreting detection data from cameras placed on roads, researchers should consider the level of human use on those roads, and how that can bias their population-level inferences from detection data.

5 | CONCLUSION

Many wildlife researchers and managers have wondered whether cameras placed on roads and trails can be used to estimate population size of unmarked animals. This is the case for many tiger conservationists, since they are already putting cameras on roads and trails to monitor tiger densities and obtain "by-catch" images of prey species in the process. Our results provide clear evidence that linear features like roads and trails bias detections of large ungulate prey species in the Russian Far East. What's more, avoidance of human activity on those roads may confound truly lower abundance of prey. Camera-based methods to estimate densities of unmarked populations assume that (i) the area sampled by cameras does not affect animal movement, and (ii) that these collective viewshed areas are representative of the study area. Based on our results, road cameras violate both of these assumptions. If managers wish to implement these methods, they should not deploy cameras on roads. While we tested a more feasible deployment strategy with off-road cameras that likely met assumption i) above, RAIs from these off-road cameras were still higher than random RAIs. Random or other representative forms of sampling remain essential to the implementation of these camera-based estimators. We strongly recommend wildlife researchers account for this when planning studies of unmarked wildlife population.

6 | LITERATURE CITED

Borkowski, J., S. C. F. Palmer, and Z. Borowski. 2011. Drive counts as a method of estimating ungulate density in forests: Mission impossible? Acta Theriologica 56:239–253.

Broadley, K., A. C. Burton, T. Avgar, and S. Boutin. 2019. Density-dependent space use affects interpretation of camera trap detection rates. Ecology and Evolution 9:14031–14041.

Buckland, S. T., E. A. Rexstad, T. A. Marques, and C. S. Oedekoven. 2015. Distance Sampling: Methods and Applications. Springer International Publishing, Cham.

Cochran, W. G. 1977. Sampling Techniques. Third edition. John Wiley & Sons, Inc.

le Cren, E. D. 1965. A Note on the History of Mark-Recapture Population Estimates. The Journal of Animal Ecology 34:453.

Cusack, J. J., A. J. Dickman, J. M. Rowcliffe, C. Carbone, D. W. Macdonald, and T. Coulson. 2015a. Random versus game trail-based camera trap placement strategy for monitoring terrestrial mammal communities. PLoS ONE 10:1–14.

Cusack, J. J., A. J. Dickman, J. M. Rowcliffe, C. Carbone, D. W. Macdonald, and T. Coulson. 2015b. Random versus game trail-based camera trap placement strategy for monitoring terrestrial mammal communities. PLoS ONE 10.

Delignette-Muller, M. L., and C. Dutang. 2015. fitdistrplus: An R Package for Fitting Distributions. Journal of Statistical Software 64:1–34.

Dou, H., H. Yang, J. L. D. Smith, L. Feng, T. Wang, and J. Ge. 2019. Prey selection of Amur tigers in relation to the spatiotemporal overlap with prey across the Sino–Russian border. Wildlife Biology 2019.

Efford, M. G., D. L. Borchers, and A. E. Byrom. 2009. Density estimation by spatially explicit capture-recapture: likelihood-based methods. Modeling demographic processes in marked populations:255–269.

Efron, B., and R. J. Tibshirani. 1993. An introduction to the Bootstrap. Chapman & Hall, New York.

Fisher, R. A. 1925. Theory of Statistical Estimation. Mathematical Proceedings of the Cambridge Philosophical Society 22:700–725.

Garton, E. O., J. S. Horne, J. L. Aycrigg, and J. T. Ratti. 2012. Research and Experimental Design. Pages 1–40 The Wildlife Techniques Manual. Seventh edition.

Gilbert, N. A., J. D. J. Clare, J. L. Stenglein, and B. Zuckerberg. 2020, February 1. Abundance estimation of unmarked animals based on camera-trap data. Blackwell Publishing Inc.

Global Tiger Initiative. 2010. Global Tiger Recovery Program 2010–2022. Page Conference Document for Endorsement.

Harihar, A., B. Pandav, M. Ghosh-Harihar, and J. Goodrich. 2020. Demographic and ecological correlates of a recovering tiger (Panthera tigris) population: Lessons learnt from 13-years of monitoring. Biological Conservation 252:108848.

Harmsen, B. J., R. J. Foster, S. Silver, L. Ostro, and C. P. Doncaster. 2010. Differential use of trails by forest mammals and the implications for camera-trap studies: A case study from Belize. Biotropica 42:126–133.

Hebblewhite, M., D. G. Miquelle, H. Robinson, D. G. Pikunov, Y. M. Dunishenko, V. V. Aramilev, I. G. Nikolaev, G. P. Salkina, I. V. Seryodkin, V. V. Gaponov, M. N. Litvinov, A. V. Kostyria, P. V. Fomenko, and A. A. Murzin. 2014. Including biotic interactions with ungulate prey and humans improves habitat conservation modeling for endangered Amur tigers in the Russian Far East. Biological Conservation 178:50–64.

Heptner, V. G., A. A. Nasimovich, and A. G. Bannikov. 1988. Mammals of the Soviet Union: Volume 1. Smithsonian Institution, Washington D.C.

Howe, E. J., S. T. Buckland, M. L. Després-Einspenner, and H. S. Kühl. 2017. Distance sampling with camera traps. Methods in Ecology and Evolution 8:1558–1565.

IUCN. 2012. IUCN Red List Categories and Criteria: Version 3.1. Page The Journal of pharmacy and pharmacology. Second edi. IUCN, Gland, Switzerland, Gland, Switzerland and Cambridge, UK.

Jaeger, J. A. G., J. Bowman, J. Brennan, L. Fahrig, D. Bert, J. Bouchard, N. Charbonneau, K. Frank, B. Gruber, and K. T. von Toschanowitz. 2005. Predicting when animal populations are at risk from roads: An interactive model of road avoidance behavior. Ecological Modelling 185:329–348.

Jhala, Y. V., Q. Qureshi, and A. K. Nayak. 2020. Status of tigers, copredators, & prey in India, 2018. New Dehli.

Johnson, A., C. Vongkhamheng, M. Hedemark, and T. Saithongdam. 2006. Effects of human-carnivore conflict on tiger (Panthera tigris) and prey populations in Lao PDR. Animal Conservation 9:421–430.

Jolly, G. M. 1979. Sampling of Large Objects. Page 194 *in* R. M. Cormack, P. P. Ganapati, and D. S. Robson, editors. Sampling Biological Populations.

Kafley, H., B. R. Lamichhane, R. Maharjan, B. Thapaliya, N. Bhattarai, M. Khadka, and M. E. Gompper. 2019. Estimating prey abundance and distribution from camera trap data using binomial mixture models. European Journal of Wildlife Research 65.

Karanth, K. U., J. D. Nichols, N. S. Kumar, W. A. Link, and J. E. Hines. 2004. Tigers and their prey: Predicting carnivore densities from prey abundance. Proceedings of the National Academy of Sciences of the United States of America 101:4854–4858.

Karanth, K. U., and James. D. Nichols. 2002. Monitoring tigers and their prey: A manual for wildlife researchers, managers and conservationists in tropical Asia. Centre for Wildlife Studies, Bangalore, India.

Kerley, L. L., A. S. Mukhacheva, D. S. Matyukhina, E. Salmanova, G. P. Salkina, and D. G. Miquelle. 2015. A comparison of food habits and prey preference of Amur tiger (Panthera tigris altaica) at three sites in the Russian Far East. Integrative Zoology 10:354–364.

Kery, M., and J. A. Royle. 2015. Applied Hierarchical Modeling in Ecology: Analysis of distribution, abundance and species richness in R and BUGS: Volume 1: Prelude and Static Models. Academic Press. Elsevier Science.

Keuling, O., M. Sange, P. Acevedo, T. Podgorski, G. Smith, M. Scandura, M. Apollonio, E. Ferroglio, and J. Vicente. 2018. Guidance on estimation of wild boar population abundance and density: methods, challenges, possibilities. EFSA Supporting Publications 15.

Kolowski, J. M., and T. D. Forrester. 2017. Camera trap placement and the potential for bias due to trails and other features. PLoS ONE 12:1–20.

Lincoln, F. C. 1930. Calculating waterfowl abundance on the basis of banding returns. United States Department of Agriculture, Washington D.C.

Matiukhina, D. 2020. Resource Partitioning and Density Drivers of Two Endangered Large Felids: Amur Tiger (Panthera tigris altaica) and Amur Leopard (Panthera pardus orientalis) in the Russian Far East. College of Environmental Science and Forestry.

Mills, L. S. 2013. Conservation of wildlife populations: demography, genetics and management. Second edition. John Wiley & Sons, Ltd., West Sussex, UK.

Miquelle, D. G., J. M. Goodrich, E. N. Smirnov, P. A. Stephens, O. Y. Zaumyslova, G. Chapron, L. Kerley, A. Murzin, M. Hornocker, and H. Quigley. 2010. The Amur Tiger: a case study of living on the edge. Pages 325–339 The biology and conservation of wild felids.

Miquelle, D. G., E. N. Smirnov, H. B. Quigley, M. G. Hornocker, I. G. Nikolaev, and E. n. Matyushkin. 1996. Food Habits of Amur Tigers in Sikhote-Alin Zapovednik and the Russian Far East, and implications for conservation. Journal of Wildlife Research 1:138–147.

Miquelle, D., W. C. Society, and P. A. Stephens. 2005. CH A P T E R 1 0 Tigers and Wolves in the Russian Far East : Competitive Exclusion , Functional Redundancy , and Conservation Implications.

Moeller, A. K., P. M. Lukacs, and J. S. Horne. 2018. Three novel methods to estimate abundance of unmarked animals using remote cameras. Ecosphere 9.

Morelle, K., J. Bubnicki, M. Churski, J. Gryz, T. Podgórski, and D. P. J. Kuijper. 2020. Disease-Induced Mortality Outweighs Hunting in Causing Wild Boar Population Crash After African Swine Fever Outbreak. Frontiers in Veterinary Science 7.

Neilson, E. W., T. Avgar, A. Cole Burton, K. Broadley, and S. Boutin. 2018. Animal movement affects interpretation of occupancy models from camera-trap surveys of unmarked animals. Ecosphere 9.

Northrup, J. M., J. Pitt, T. B. Muhly, G. B. Stenhouse, M. Musiani, and M. S. Boyce. 2012. Vehicle traffic shapes grizzly bear behaviour on a multiple-use landscape. Journal of Applied Ecology 49:1159–1167.

O'Brien, T. G. 2011. Abundane, Density, and Relative Abundance: A Conceptual Framework. Page *in* A. F. O'Connell, James. D. Nichols, and K. U. Karanth, editors. Camera Traps in Animal Ecology. Springer, Tokyo, Japan.

Palencia, P., J. M. Rowcliffe, J. Vicente, and P. Acevedo. 2021. Assessing the camera trap methodologies used to estimate density of unmarked populations. Journal of Applied Ecology 58:1583–1592.

Qi, J., J. Gu, Y. Ning, D. G. Miquelle, M. Holyoak, D. Wen, X. Liang, S. Liu, N. J. Roberts, E. Yang, J. Lang, F. Wang, C. Li, Z. Liang, P. Liu, Y. Ren, S. Zhou, M. Zhang, J. Ma, J. Chang, and G. Jiang. 2021. Integrated assessments call for establishing a sustainable meta-population of Amur tigers in northeast Asia. Biological Conservation 261:109250.

Raudenbush, S.W., and A.S. Bryk. 2002. Hierarchical linear models: Applications and data analysis methods (Vol. 1). sage.

Roever, C. L., M. S. Boyce, and G. B. Stenhouse. 2010. Grizzly bear movements relative to roads: Application of step selection functions. Ecography 33:1113–1122.

Rowcliffe, J. M., J. Field, S. T. Turvey, and C. Carbone. 2008. Estimating animal density using camera traps without the need for individual recognition. Journal of Applied Ecology 45:1228–1236.

Royle, J. A. 2004. N-Mixture Models for Estimating Population Size from Spatially Replicated Counts. Page Biometrics.

Royle, J. A., J. D. Nichols, K. U. Karanth, and A. M. Gopalaswamy. 2009. A hierarchical model for estimating density in camera-trap studies. Journal of Applied Ecology 46:118–127.

Sollmann, R., A. Mohamed, H. Samejima, and A. Wilting. 2013. Risky business or simple solution - Relative abundance indices from camera-trapping. Biological Conservation 159:405–412.

Steinhorst, R. K., and M. D. Samuel. 1989. Sightability Adjustment Methods for Aerial Surveys of Wildlife Populations. Biometrics 45:415–425.

Stephens, P. A., O. Y. Zaumyslova, G. D. Hayward, and D. G. Miquelle. 2006. Analysis of the long-term dynamics of ungulates.

Tanwar, K. S., A. Sadhu, and Y. V. Jhala. 2021. Camera trap placement for evaluating species richness, abundance, and activity. Scientific Reports 1 1.

Tempa, T. 2017. The ecology of montane bengal tigers (Panthera tigris tigris) in the Himalayan Kingdom of Bhutan. University of Montana.

Tempa, T., M. Hebblewhite, J. F. Goldberg, N. Norbu, T. R. Wangchuk, W. Xiao, and L. S. Mills. 2019. The spatial distribution and population density of tigers in mountainous terrain of Bhutan. Biological Conservation 238:108192.

Thurfjell, H., G. Spong, M. Olsson, and G. Ericsson. 2015. Avoidance of high traffic levels results in lower risk of wild boar-vehicle accidents. Landscape and Urban Planning 133:98–104.

Vistnes, I., and C. Nellemann. 2001. Avoidance of Cabins, Roads, and Power Lines by Reindeer during Calving. Page Source: The Journal of Wildlife Management.

Williams, B. K., J. D. Nichols, and M. J. Conroy. 2002. Analysis and Management of Wildlife Populations. Academic Press.

Xiao, W., M. Hebblewhite, H. Robinson, L. Feng, B. Zhou, P. Mou, T. Wang, and J. Ge. 2018. Relationships between humans and ungulate prey shape Amur tiger occurrence in a core protected area along the Sino-Russian border. Ecology and Evolution 2018:1–17.

7 | TABLES & FIGURES

Table 2-1. Summary of the seasons and number of cameras (N) for the comparison of RAIs between road, off-road, and random cameras. The dates of the years are as follows: 2019-20 (February 10 – April 10, 2020); 2020-21 (October 10 – December 10, 2020); 2020-21 (TBD). For the road and off-road cameras, the left value describes the number of cameras used in the road-off-road comparison as opposed to the southern study area comparison only on the right. For instance, "31 | 14" indicates that 31 road cameras were used for the road / off-road comparison, but only 14 road cameras were used in the road / off-road / random comparison.

Study area	Year	N road	N off-road	N random
SABZ	2019-20	0	31 | 14	35
SABZ	2020-21	31 | 14	31 | 14	36
UL Nat'l Park	2020-21	19	19	NA
Sidatun	2021-22	30	30	NA
Confirmed total:		**80 | 14**	**111 | 28**	**71**

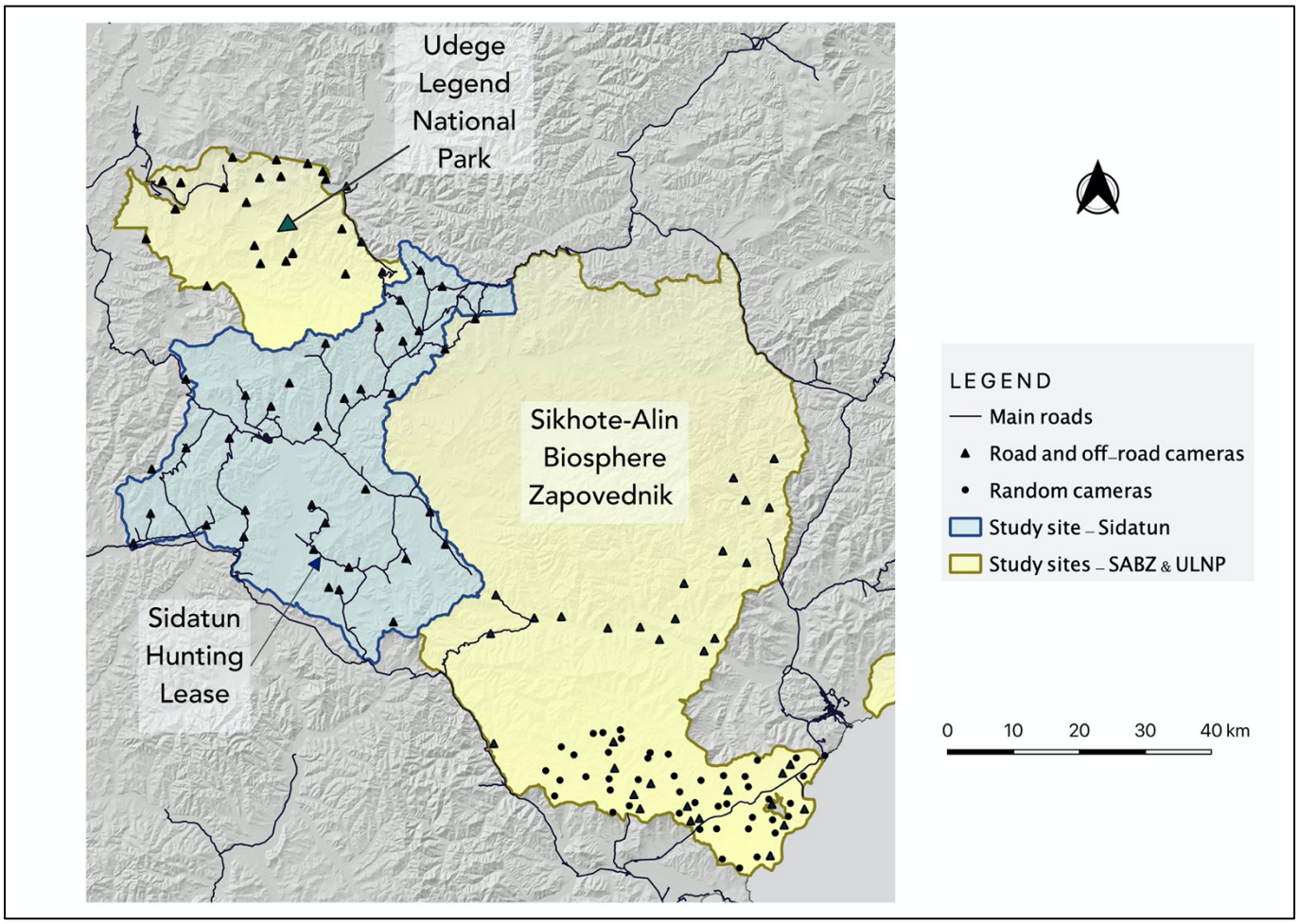

Figure 1. Study sites within Central Sikhote-Alin, Russian Far East. Sikhote-Alin Biosphere Zapovednik (SABZ) and Udege Legend National Park (ULNP) are both protected areas and are colored yellow. Sidatun Hunting Lease (Sidatun) is represented in blue. Road and off-road cameras are in triangle shape, while random cameras are circles. Note that the locations between Seasons 1, 2, and 3 for random and off-road cameras varied. Here we have combined road and off-road locations and presented only random locations from Season 3 for simplicity.

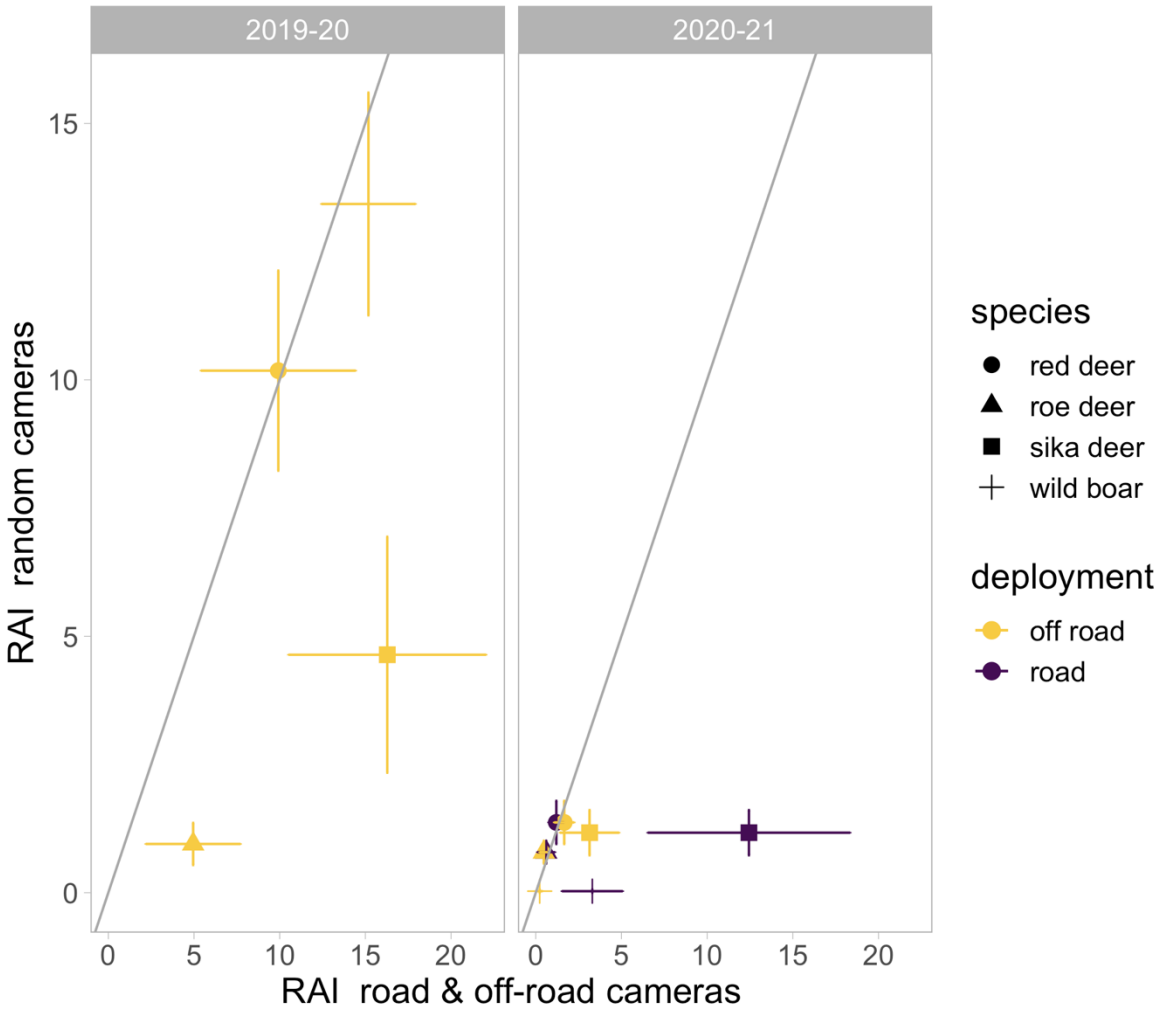

Figure 2-2. Comparisons of relative abundance indices (RAIs) for road and off-road cameras compared to random cameras. RAIs are the median of an exponential distribution fitted to camera-specific RAIs using maximum likelihood estimation. Error boars indicate standard error of the median RAI using 1001 iterations of nonparametric bootstrapping.

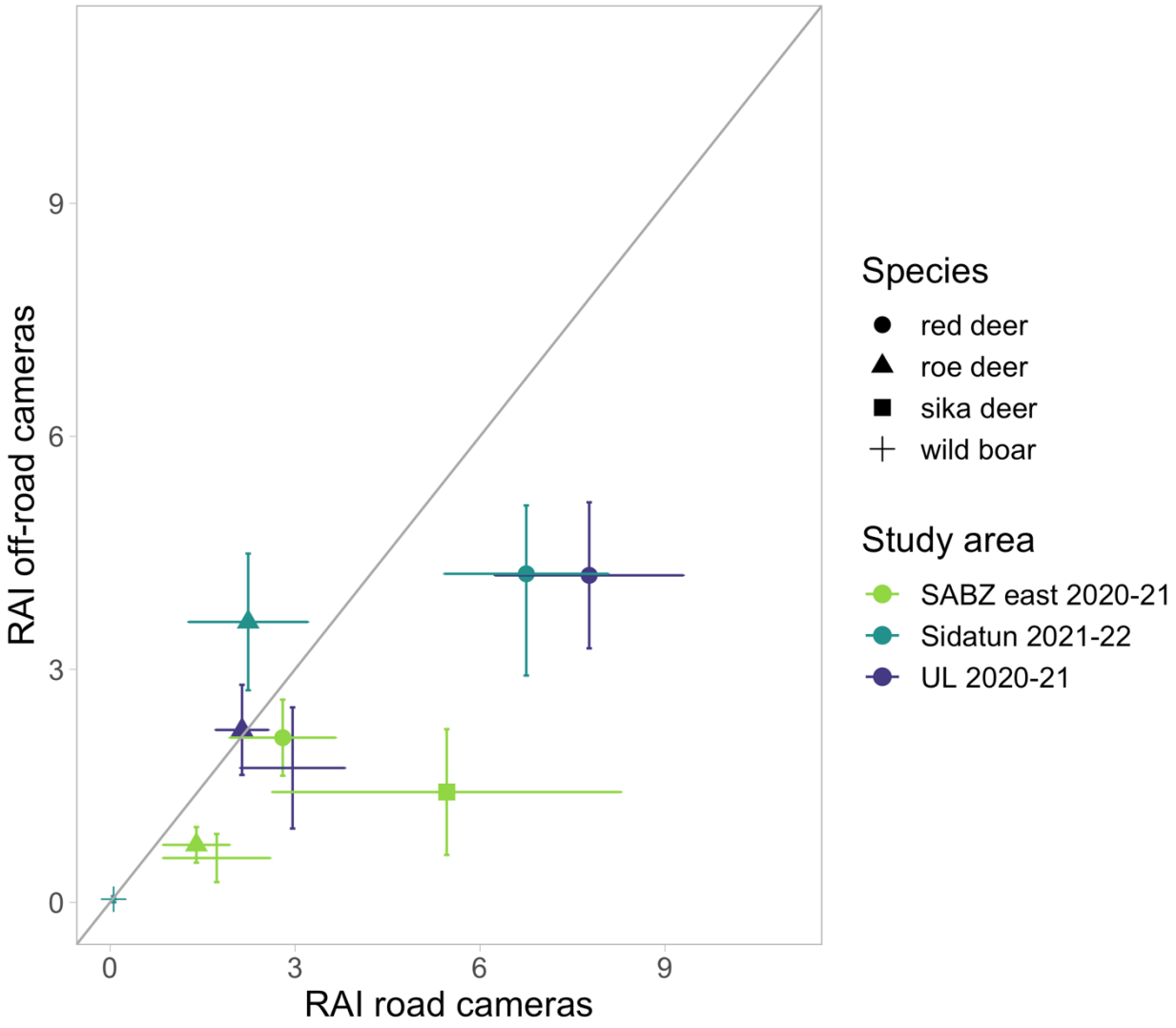

Figure 2-3. Comparisons of relative abundance indices (RAIs) between road and off-road cameras for 3 seasons in Sikhote-Alin Zapovednik (SABZ), as well as the Sidatun hunting lease and Udege Legend National Park (UL). RAIs are the median of an exponential distribution fitted to camera-specific RAIs using maximum likelihood estimation. Error boars indicate standard error of the median RAI using 1001 iterations of nonparametric bootstrapping.

Table 2-2. Summary results from the linear mixed-effects model testing for significant differences in bootstrapped RAIs between random (the intercept, β_0, in the regression model), road, and off-road cameras deployed in a southern study area in the Sikhote-Alin Biosphere Zapovednik. We used a random intercept for year to account for differences in RAIs for a given species between years. Asterisks indicate a significance level of $p < 0.05$.

Model formula	Species	Parameter	Estimate	SE	*p*
RAI ~ deployment + (1 | year)	Wild boar	Random (β_0)	6.70	7.02	
		Road	2.12	0.07	$p < 0.001$*
		Off-road	0.92	0.05	$p < 0.001$*
	Red deer	Random (β_0)	5.77		
		Road	1.30	0.09	$p < 0.001$*
		Off-road	-0.00	0.07	$p = 0.99$
	Roe deer	Random (β_0)	0.87	1.13	
		Road	1.66	0.07	$p < 0.001$*
		Off-road	1.79	0.05	$P < 0.001$*
	Sika deer	Random (β_0)	2.84	4.06	
		Road	6.49	0.16	$P < 0.001$*
		Off-road	6.84	0.12	$P < 0.001$*

Table 2-3. Summary results from the linear mixed-effects model testing for significant differences in bootstrapped RAIs between off-road (the intercept, β_0, in the regression model), and road cameras deployed during two different years in eastern Sikhote-Alin Zapovednik, and one year each in Sidatun hunting lease and Udege Legend National Park . We used a random intercept for study area to account for differences in RAIs between study areas. Asterisks indicate a significance level of $p < 0.05$.

Model formula	Species	Parameter	Estimate	SE	*p*
RAI ~ deployment + (1 | study area)	Wild boar	Off-road (β_0)	1.17	0.59	
		Road	1.22	0.02	$p < 0.001$*
	Red deer	Off-road (β_0)	3.19	1.72	
		Road	2.03	0.04	$p < 0.001$*
	Roe deer	Off-road (β_0)	1.46	0.55	
		Road	0.30	0.02	$p < 0.001$*
	Sika deer	Off-road (β_0)	1.42	0.14	
		Road	3.85	0.09	$P < 0.001$*

Table 2-4. Results from categorical regression testing for a significant effect of high human traffic (> 75 vehicles / 100 days) on prey RAIs. Regression results are reported for each prey species. We did not include sika deer because they are virtually absent from our two study areas of Sidatun hunting lease and Udege Legend National Park. We also included the effects on a combined prey index (the sum of individual prey RAIs). Asterisks indicate a significance level of $p < 0.05$.

Model formula	Species	Parameter	Estimate	SE	*p*
RAI ~ traffic_binary	Wild boar	Low traffic (β_0)	11.85	1.34	
		High traffic	-5.24	4.43	$p = 0.24$
	Red deer	Low traffic (β_0)	10.19	0.72	
		High traffic	-5.66	2.36	$p = 0.02$*
	Roe deer	Low traffic (β_0)	2.74	0.25	
		High traffic	1.37	0.83	$p = 0.10$
	Combined prey	Low traffic (β_0)	26.32	1.74	
		High traffic	-10.67	5.76	$p = 0.06$

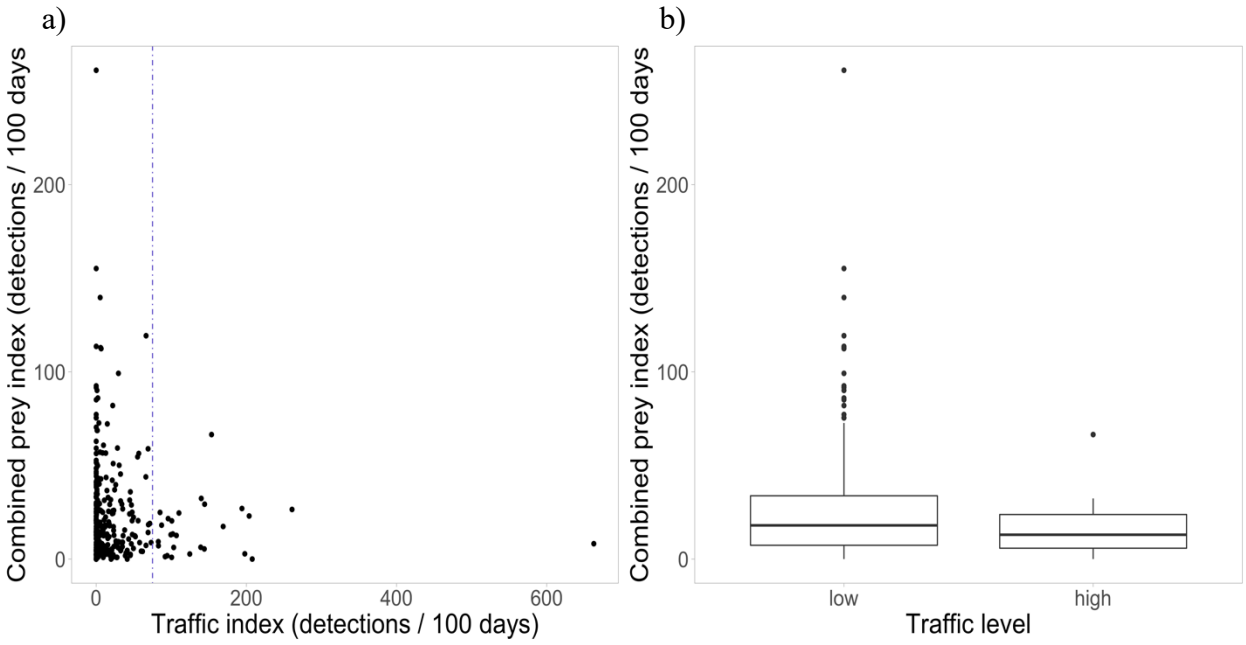

Figure 2-4. (a) Scatter plot showing the relationship between the combined human traffic index at road cameras, and a combined prey index (the sum of all prey species' RAIs). Data are combined from 295 camera locations across 3 years and 4 study areas (Sikhote-Alin Biosphere Zapovednik, Udege Legend National Park, Sidatun hunting lease, and Terney hunting lease, east of Sikhote-Alin Zapovednik). The dashed line indicates the traffic index (75) which divided our categories of traffic as low (≤ 75 vehicles / 100 days) or high (> 75 vehicles / 100 days). (b) Box plots showing the distribution of combined prey RAIs at roads categorized as having either low or high human traffic.